Construction and Building Materials 402 (2023) 132996

Contents lists available at ScienceDirect

Construction and Building Materials

journal homepage: www.elsevier.com/locate/conbuildmat

Review

Autoclaved aerated concrete masonry for energy efficient buildings: State of the art and future developments

Elena Michelini [a], Daniele Ferretti [a], Lorenzo Miccoli [b], Fulvio Parisi [c,*]

[a] Department of Engineering and Architecture, University of Parma, Parco Area delle Scienze 181/A, 43124 Parma, Italy
[b] Department of Applied Research/Building Physics, Xella Technologie- und Forschungsgesellschaft mbH, 14797 Kloster Lehnin, Germany
[c] Department of Structures for Engineering and Architecture, University of Naples Federico II, Via Claudio 21, 80125 Naples, Italy

ARTICLE INFO

Keywords:
Autoclaved aerated concrete
Energy efficient buildings
Sustainable concrete masonry
Mechanical properties
Thermal insulation

ABSTRACT

The pressing demand for green buildings poses new challenges to the construction sector. In this context, an effective strategy to be pursued is represented by the use of construction materials with enhanced thermal properties, together with a reduced carbon footprint and adequate structural resistance. Autoclaved Aerated Concrete (AAC) masonry is one of the most interesting solutions. Several studies have been published so far to investigate the influence of raw materials and production processes on the macroscopic properties of AAC blocks. This paper aims to refine and extend the literature review on AAC, by collecting and processing experimental data related not only to the material itself, but also to masonry assemblages. In order to span different aspects of sustainable design, a comprehensive review on both physical and mechanical properties (related to safety issues) as well as thermal properties (related to environmental aspects) of AAC is provided. This study shows how constituent materials influence the macroscopic behavior of AAC masonry, also comparing experimental trends with relationships suggested in European design standards.

1. Introduction

The European Green Deal has favored the spread of a new sensibility towards climate change adaptation and the urgent need to reduce CO_2 emissions [1]. The development of sustainable constructions is vital in this regard, due to the huge carbon footprint of traditional materials (such as normal concrete, clay bricks, steel, etc.) and technologies used in the construction industry till now. If the data published on the European Commission official website is considered, approximately 5% to 12% of total national greenhouse gas (GHG) emissions derive from the operations connected to building construction and renovation, together with related processes for manufacturing of construction materials [2]. Another threat to the climate comes from the normal functioning of buildings that consumes up to 40% of the EU's energy requirements, just for indoor heating and cooling [3–5]. In addition, up to 35% of total waste generation in Europe can be related to the building sector. It is estimated that 80% of GHG emissions could be saved by simply pursuing greater material efficiency [2]. Within this context, Autoclaved Aerated Concrete (AAC) can represent an interesting solution for different reasons. AAC was first developed in Sweden in the 1920s by Eriksson, who patented the process for producing an aerated mixture of limestone and ground slate. A few years later, Eriksson introduced autoclaving into the production process, which greatly improved the properties of the final material. The first factory for large-scale production of AAC was established in Sweden in 1929, and after the Second World War, AAC suppliers expanded in different European countries. During the 1980s and the 1990s, several plants were also built in Eastern Europe, Asia, and the Middle East, implementing different production processes. Since then, great strides have been made to improve the properties of AAC [6]. The main advantages offered by AAC with respect to normal concrete blocks and clay bricks are basically related to its porous structure, and in turn to its reduced density. Due to its porous but also homogenous structure, AAC shows lower values of thermal conductivity and ensures good sound insulation when compared to most concretes and clay bricks [7–16]. This configuration is also beneficial in terms of fire resistance [17].

Thanks to its inherent thermal insulation and high durability [18], AAC can meet the increasingly stringent requirements on energy efficiency, building comfort and sustainability (in terms of reduction of carbon emissions). Fig. 1 plots the improvement in the last decades of the thermal conductivity values for AAC blocks with three different values of compressive strength f_b. For example, Fig. 2 shows the improvement of thermal transmittance values achieved in last decades

* Corresponding author.
E-mail address: fulvio.parisi@unina.it (F. Parisi).

https://doi.org/10.1016/j.conbuildmat.2023.132996
Received 27 May 2023; Received in revised form 12 August 2023; Accepted 14 August 2023
Available online 24 August 2023

Nomenclature

A_i	cross-sectional area of masonry samples parallel to bed joints (mm^2);
b	width/height of masonry units (mm);
E	short-term secant modulus of elasticity of masonry (MPa);
E_c	secant modulus of elasticity of AAC material (MPa);
f_b	normalized mean compressive strength of masonry units (MPa);
$f_{bt,cal}$	calculated tensile strength of masonry units (MPa);
f_{ck}	characteristic compressive strength of cubic specimens (MPa);
f_{cp}	compressive strength of prismatic specimens (MPa);
$f_{c,cores}$	compressive strength of core specimens (MPa);
$f_{t,flk;\ 0,05}$	characteristic value defined as 5th quantile of flexural strength of AAC material (MPa);
$f_{t,flk;\ 0,95}$	characteristic value defined as 95th quantile of flexural strength of AAC material (MPa);
f_{cr}	masonry cracking stress (MPa);
f_k	characteristic compressive strength of masonry (MPa);
f_i	compressive strength of single masonry specimen (MPa);
$f_{i,min}$	minimum compressive strength of masonry specimens (MPa);
f_{mean}	mean compressive strength of masonry (MPa);
f_{pi}	precompression stress of single masonry specimen (MPa);
f_{st}	converted value of the compressive strength class (MPa);
f_t	direct tensile strength of AAC material (MPa);
$f_{t,fl}$	modulus of rupture of AAC material (MPa);
$f_{t,spl}$	splitting tensile strength of AAC material (MPa);
f_u	mass-related moisture conversion coefficient (-);
f_{v0i}	shear strength of single masonry specimen (MPa);
f_{vk}	characteristic shear strength of masonry (MPa);
f_{vk0}	characteristic initial shear strength of masonry under zero compressive stress (MPa);
f_{vlt}	upper-bound value of f_{vk} (MPa);
$f_{x,mean}$	mean value of flexural strength of masonry (MPa);
f_{xi}	flexural strength of single masonry specimen (MPa);
f_{xk}	characteristic value of flexural strength of masonry (MPa);
f_{xk1}	characteristic value of flexural strength parallel to bed joints (MPa);
f_{xk2}	characteristic value of flexural strength perpendicular to bed joints (MPa);
$F_{max,i}$	ultimate load of single masonry specimen (N);
F_{pi}	precompression load on single masonry specimen (N);
G_F	fracture energy of AAC material (N/m);
k	factor depending on the number n of specimens (-);
K	constant for calculation of the compressive strength of masonry (-);
K_E	coefficient for calculation of the Youngs modulus of masonry (-);
l_1	distance between axes of outer load transmission (mm);
l_2	distance between axes of inner load transmission (mm);
l_{ch}	characteristic length (mm);
m	moisture content ($M.$-%);
s	standard deviation (*measurement unit of selected property*);
t_u	thickness of masonry (mm);
U	thermal trasmittance ($W/(m^2 \cdot K)$);
y_{mean}	mean value of flexural strength of masonry specimens (MPa);
w	crack opening width (mm);
ε_i	axial strain (shortening) at one third of ultimate strength (-);
λ	thermal conductivity ($W/(mK)$);
$\lambda_{10,dry}$	thermal conductivity in dry condition ($W/(mK)$);
λ_d	design thermal conductivity ($W/(mK)$);
λ_R	calculation value of thermal conductivity ($W/(mK)$);
ρ	dry bulk density (kg/m^3);
σ_d	design compressive stress (MPa).

for AAC buildings, in case of blocks with $f_b \geq 2.5$ MPa and thickness $t_u =$ 365 mm.

An increased use of AAC in new projects, as well as in renovation works, can therefore represent a good strategy to significantly decrease the energy consumption of the European building stock in the short term, by also reducing the use of additional insulation materials

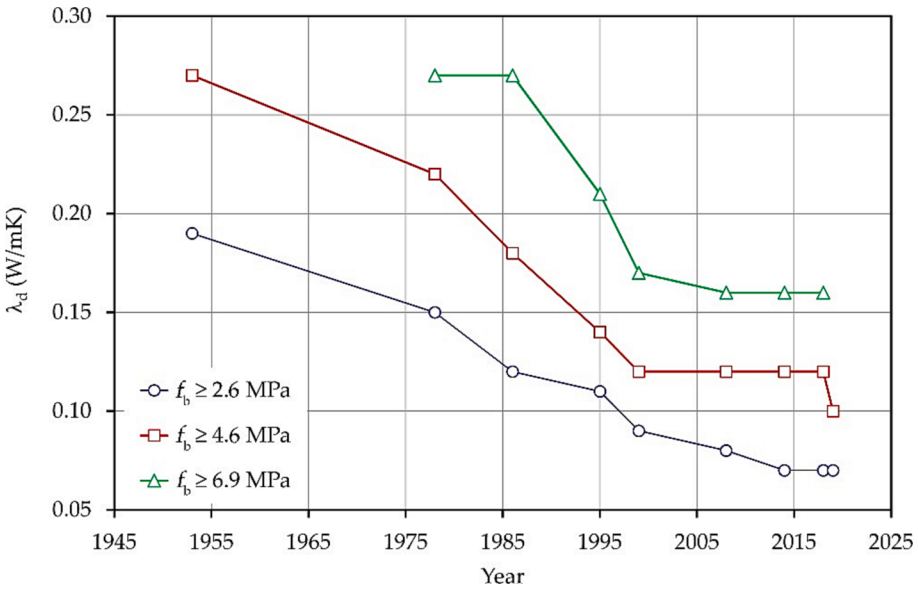

Fig. 1. Improvement of thermal conductivity values λ_d for three different AAC block types in the last decades [source: Xella Technologie- und Forschungsgesellschaft mbH]. Compressive strength f_b reported according to DIN 20000–404 [24].

[5,19–21]. However, while in the past decades the focus was almost exclusively aimed at measures that reduce the heating energy and energy demand of buildings, in the coming years greater attention will be paid to a building's CO_2 footprint over its entire life cycle [22]. According to Walther [23], the absolute reduction of the carbon footprint or global warming potential (GWP) of AAC through recarbonation during the use phase is directly associated with the amount of binder (cement, quicklime) used. The impact of recarbonation on total AAC carbon emissions is documented in an Environmental Product Declaration (EPD) independently verified by the German Institut Bauen und Umwelt (IBU) using data sourced from a representative AAC factory in 2020.

Another interesting aspect in view of sustainability is related to the easy workability of AAC that allows accurate cutting operations, and the use – as for other modern masonry system made of clay bricks – of thin mortar layers (from 1 to 3 mm). This guarantees an increase in construction speed, a reduction of heat losses through mortar joints, and above all, a reduction of solid wastes during construction and operation [5]. In addition, AAC wastes can be largely recycled, hence minimizing the environmental impact related to their storage in landfills [5,25–28].

Going back again to the lighter weight of AAC, such a physical property allows economic savings during transportation and construction stages, as well as a reduction in the dead load of buildings, with obvious favorable effects on foundations and seismic behavior [7,29]. Despite its lightness, AAC still provides good structural performances, and blocks with $\rho = 250$–$650\ kg/m^3$ are successfully adopted for load-bearing masonry in different constructions such as residential and commercial buildings, hospitals, and offices [12,30,31]. As discussed in [32–35], unreinforced AAC masonry can be also used in seismic-prone areas using blocks with $\rho \geq 350\ kg/m^3$ (ETA 17/0365, [36]). Buildings with regular geometry are indeed able to withstand low-to-medium intensity earthquakes without significant damage [37]. In high-seismicity areas, other solutions like confined masonry or bed-joint reinforced walls should be however preferred. Moreover, infill walls made of AAC masonry are used in seismic areas where the bearing structure consists of reinforced concrete or steel frames. Thanks to this combination of good mechanical performances, high thermal insulation and environmental friendly characteristics, the AAC production market is anticipated to rise at a considerable rate in the near future, which was expected to start from 18.43 billion dollars in 2020 and to reach 29.55 billion in 2027 [38].

The aim of this work is to provide a broad focus on AAC masonry and its components, their main properties, and guidelines for testing and design according to relevant Standard Codes within the European context. Except for the research works carried out in the standardization committees and for the approval of specific AAC masonry components, most of review works published so far only deals with the characteristics of the raw material (e.g. [7,39–41]). This work presents a comprehensive analysis of data on AAC, starting with an overview of the main mechanical and thermal properties of AAC blocks, for their use in design calculations and numerical modelling of AAC structures (especially by means of finite element analyses). Subsequently, the attention is focused on the behavior of AAC masonry, trying to highlight the influence of constituents on the global behavior of the masonry assemblage. At the same time, the main regulatory guidelines for both testing and design calculations are reviewed. The purpose of the work is to collect, systematically process and discuss the available knowledge and experimental data on AAC masonry at both constituent and assemblage scales, in order to support sustainable design and retrofit of AAC masonry components and structures. This study is deemed useful not only as a basis for drafting technical guidelines for designers and practitioners, but also to compare different methodologies used in different countries, allowing the identification of their strengths and weaknesses. In this respect, this study is expected to support the activity of fib Task Group 7.7 "Sustainable concrete masonry components and structures" of the Fédération Internationale du Béton, as well as standardization committees at both national and international levels.

2. General overview on autoclaved aerated concrete

Autoclaved aerated concrete belongs to the category of lightweight concretes, with a density ρ usually ranging between 250 and 650 kg/m^3 [39,41–43]. Its lightness directly derives from the microstructure of the material, which is characterized by a high total porosity, up to 85% of the hardened phase by volume [39,42,44]. The presence of air voids uniformly distributed in the framework consisting mainly of calcium silicate hydrate phases, in particular tobermorite-11Å, is obtained through the addition of an expanding agent – usually aluminum powder – to the slurry, during the manufacturing process [39,45–48]. Air pores have an almost spherical shape, with a diameter usually variable between 0.5 and 3 *mm*, and a mutual distance ranging between zero (interconnected or adjacent pores) and 1 mm [42,49,50], as shown in

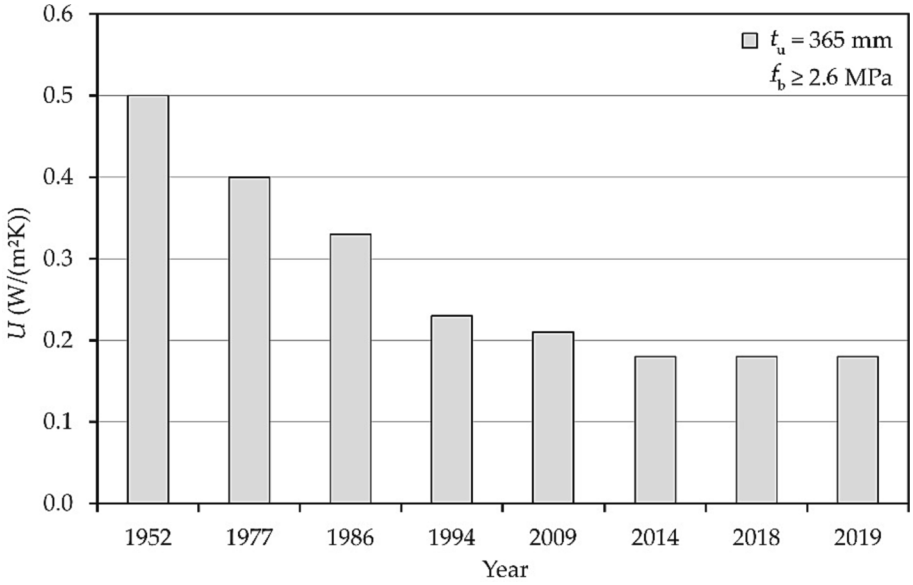

Fig. 2. Improvement of thermal transmittance values U of AAC buildings using blocks with compressive strength $f_b \geq 2.5\ MPa$ and thickness $t_u = 365\ mm$ in the last decades [source: Xella Technologie- und Forschungsgesellschaft mbH].

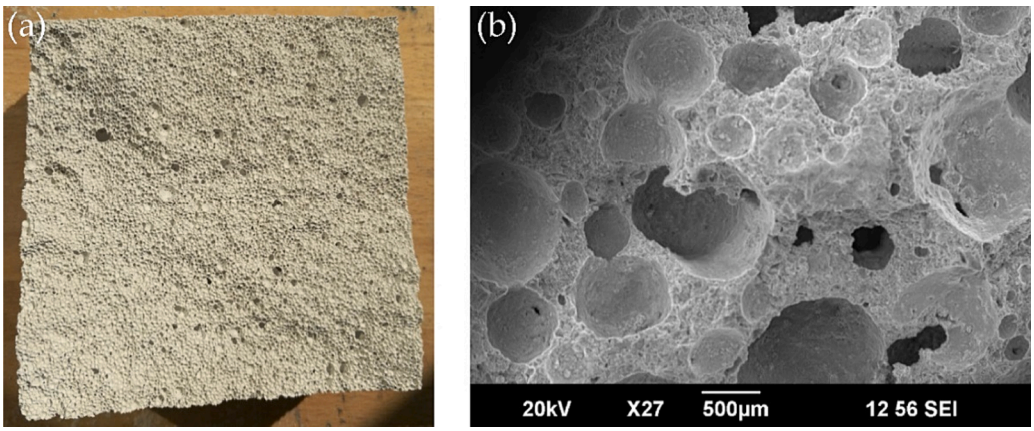

Fig. 3. Porous structure of AAC: (a) based on visual inspection, and (b) from output of Scanning Electron Microscope (SEM) [source: Xella Technologie- und Forschungsgesellschaft mbH].

Fig. 3.

Pore size and pore distribution depend on the type of expanding agent and its dosage, which can be varied to obtain products with different values of ρ. Concerning the European market, blocks with ρ = 250–350 kg/m^3 are used for infills and claddings, and blocks with ρ = 250–650 kg/m^3 are used for load-bearing masonry. In the Asian market, also blocks with ρ = 800 kg/m^3 can be found. Concerning AAC prefabricated elements, densities ρ = 400–600 kg/m^3 are commonly used for elements with structural reinforcements. In the absence of structural reinforcement, AAC prefabricated elements with ρ = 350 kg/m^3 can be adopted.

The typical raw materials used for production of AAC are cement, lime, either silica or milled quartz sand, and water [39,40,44–47,51]. AAC does not contain coarse aggregates, and consequently its structure is relatively homogeneous [52]. Gypsum or anhydrite is often added to the admixture with a function of regulator agent in the gassing process, since it acts on the hardening speed of the slurry and on the hydration process of quicklime [53]. The addition of gypsum accelerates indeed the formation of tobermorite-11Å during the autoclaving process, improving some properties of finished products [54]. As already observed, the cellular structure of the final product is obtained through the addition of an aluminum paste or powder, which leads to the formation of small hydrogen bubbles into the slurry [8,55–57]. Subsequent autoclaving of the material at high temperature (180–190°C) and pressure imparts strength, dimensional stability, and other properties to the hardened final product [52,58–61]. Typically, the duration of the autoclaving treatment may vary between 8 and 16 *h*, whereas pressure may range between 11 and 16 *bar* [7,39,62].

In the last 20 years, an increasing interest in the possible use of alternative materials (mainly coming from agricultural and industrial wastes) has been recorded in the production process of AAC. Since AAC with fly ash (FA) is already available from many years, in the last decades mine tailings, copper or iron tailings, municipal solid waste incineration (MSWI) bottom ash, coal bottom ash (CBA), silica fume (SF), granulated blast furnace slag (GBFS), air-cooled slag (ACS), slate waste, glass or perlite waste, zeolite, rice husk, bagasse ash, and also recycled AAC waste have been used in partial replacement of sand [25,46,52,63–79]. Some studies have recently explored the use of alkali activated slag (AAS), or palm-oil fuel ash, as an alternative to Portland cement [80,81]. Other works discussed the possibility of partially replacing aluminum powder with either MSWI bottom ash or aluminum dust [46,56]. The potential for large-scale use of industrial by-products in the production process of AAC is another interesting aspect that meets several objectives of the 2030 Agenda for Sustainable Development approved by the United Nations General Assembly [82], from the saving of unrenewable resources to the reduction of energy consumption, a more rational waste disposal, and a reduction of landfill activity. Recent studies [28,83] have also shown that closed-loop recycling of post-demolition AAC in AAC production has a high potential for mitigation of environmental impact. In addition, post-demolition AAC can be successfully used in the production of lightweight aggregate concrete, lightweight mortar and shuttering blocks made with no-fines concrete. All these aspects contribute to a significant reduction of production costs. Most of these 'green' applications have been already discussed in recently published review papers, to which reference is made for further details (i.e. [7,40,44,65,84,85]).

3. Key properties of AAC

3.1. Standards for material testing

The European standards EN 771-4 [47] and EN 12602 [86] provide information on the main properties of AAC blocks and reinforced AAC with regards to test methods and declared properties. Material tests on blocks have to be performed for characterization of compressive strength (EN 772-1 [87]), dry bulk density (EN 772-13 [88]) and moisture content (EN 772-10 [89]) of AAC units. In addition, the values of Young's modulus (EN 1352 [90], ASTM C-469 [91]), flexural strength (EN 1351 [92], ASTM C-78 [93]), bond strength (EN 1015-12 [94], EN 1052-3 [95]), drying shrinkage (EN 680 [96]), thermal conductivity $\lambda_{10,dry}$ (EN 12664 [97], EN 1745 [98]) and sorption moisture (EN ISO 12571 [99], EN 772-11[100]) can be detected when required by the compilation of declaration of performance or technical data sheets.

3.2. Bulk density

Material density ρ is strictly related to porosity, and consequently it is usually varied by acting on the dosage of the expanding agent and also the water/solid ratio of the raw material formulation [39,40,42,101]. Apart from the amount of pores and their size, it is also important to control pore distribution within the material [102]: a uniform pore distribution is indeed essential to obtain a final product with uniform density. It is reported that also autoclaving conditions have a limited influence on material density, due to the formation of a larger amount of hydrated products in case of longer durations of the treatment [103,104].

The declared density of AAC units refers to the oven-dried material tested according to EN 771-4 [47]. The actual density of AAC blocks when delivered at the building site is higher, because it is dependent on the moisture content. At the end of the autoclaving process, moisture content usually ranges between 20% and 35% by weight (depending on the water/solid ratio of the raw material formulation), while it reduces up to 3–6% by weight after one or two years in equilibrium with the typical environmental conditions [58].

3.3. Compressive strength

As other mechanical properties, compressive strength is dependent on material density ρ. Although it is not always possible to define a strict relationship between compressive strength and bulk density, the German standard DIN 20000-404 [24] proposes a correspondence table where, for different ranges of ρ values, compressive strength classes of the blocks are associated. Differently from other properties (flexural tensile strength, fracture energy, elastic modulus) that show an almost linear trend with density, the relation between compressive strength and density is found to be exponential [16,42,101,105]. Fig. 4 shows the range of variation for compressive strength as a function of ρ for AAC blocks available in the European market.

The variability of compressive strength for a given ρ value is not surprising, if we take in mind that this mechanical property is affected by a lot of factors. For this reason, most of correlations between compressive strength and density available in the literature (for example [101,106,107]), which were calibrated on single experimental programs, can be hardly generalized to different material productions [16].

First of all, compressive strength obviously decreases with increasing porosity, while for a similar porosity an increment of larger pores leads to lower strength values [14,40,42,62,63,103,108,109]. Compressive strength also decreases with a decreasing thickness of pore walls, which in turn depends on the mutual distance between pores [101]. Compressive strength is strictly related to the amount and degree of crystallinity of the final hydrated products (mainly a stable form of tobermorite-11Å), and consequently it depends on the type and proportioning of raw materials used in the production process, water dosage, as well as autoclaving conditions (in terms of duration, pressure and temperature) [7,46,108,110]. The CaO-to-SiO_2 ratio (controlled by the dosage of the raw materials cement/quicklime and sand) should be preferably kept in the range 0.8–1.0, to prevent the inhibition or decomposition of tobermorite phase, as reported in [40]. Although the previous statement is not valid for all types of AAC, in principle, it is important to adapt the binder content to the sand fineness in order to obtain the compressive strength required for the application.

Other factors influencing the measured values of compressive strength are the size and shape of specimens, the testing and curing conditions, the moisture content at the time of testing, and the direction and speed of loading [111–115]. Conversion factors are used in testing and product standards to take the effects of these variables into account. As concerns the specimen geometry, most of the Standard Codes (like for example [87]) prescribe the use of cubic specimens with an edge length of 100 *mm*, even if RILEM recommendations also allow the use of either cubes with other sizes (typically 150 *mm*) or cylindrical/prismatic specimens, providing that the strength determined on such specimens can be directly related to that determined on 100-*mm* cubes [62] (Fig. 5a).

Based on experimental results, cylindrical/prismatic specimens provide lower strength values with respect to cubes (approximately 5% lower, for slenderness equal to 2–3 [62,116,117]) and are characterized by a different crack pattern at failure (Fig. 5b). According to the

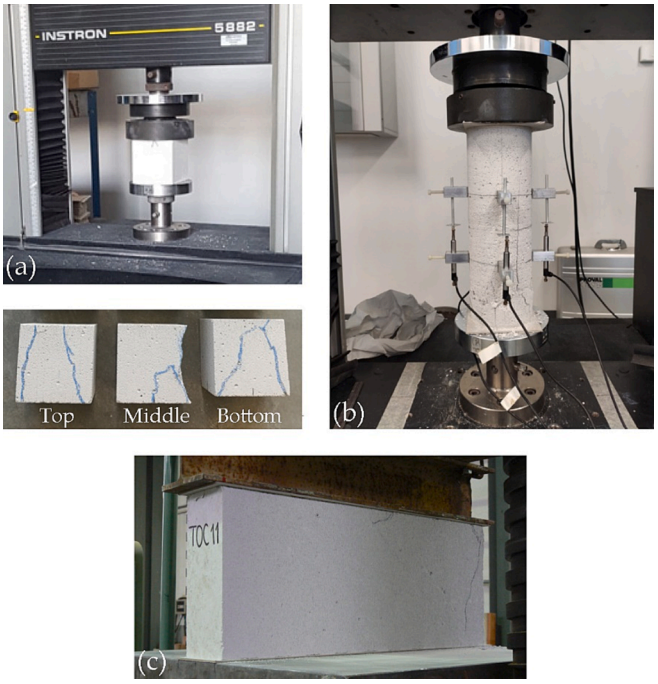

Fig. 5. Compression tests on (a) cubic specimens, (b) cylindrical specimens, and (c) blocks, with the corresponding crack patterns at failure.

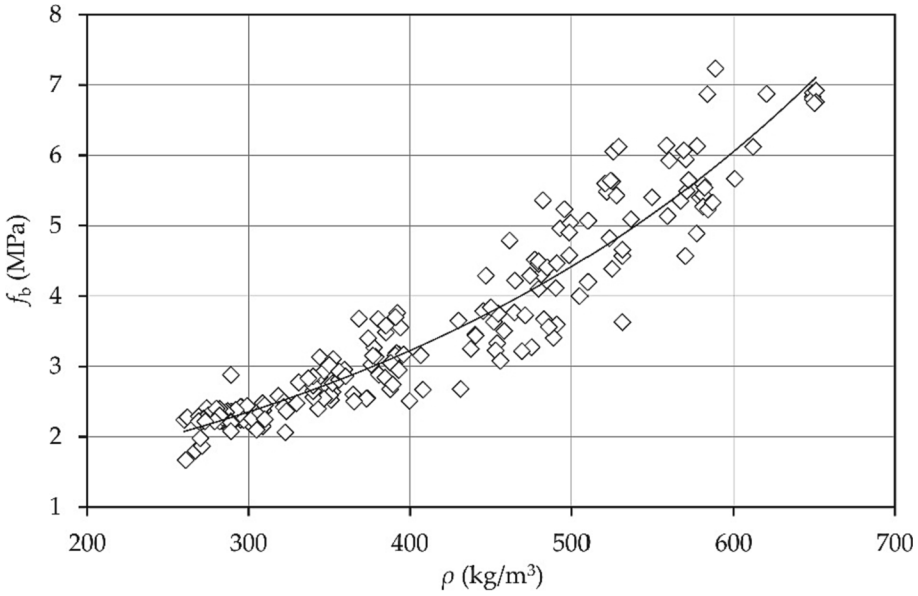

Fig. 4. Range of variation of compressive strength vs. dry density of AAC blocks used in the European market [source: Xella Technologie- und Forschungsgesellschaft mbH].

European norm EN 771-4 [47], compressive strength for measurements on cubes is always determined on three cubes, evenly distributed over the length of the block. This representative value also takes into account the influence of the rising height. Compressive strength measured directly on block units may be up to 20% lower than those measured on cubes [62,114,118], because in this case the maximum load is governed by the failure of the weaker side of the specimen according to the rising direction of the material (Fig. 5c). It is known that the compressive strength in the rising direction is about 10–15% lower than that measured in the perpendicular direction [62,101]. Therefore, it is important that the loading direction during compression tests is consistent with the direction of the compression force in use. Relatively to the loading speed, it has been observed that a reduced loading rate is associated with a decrease in the ultimate load [119]. Usually, tests should be carried out at the loading rate specified by relevant standard codes as a function of the expected compressive strength of the specimen (see for example [87]). The behavior of AAC specimens under a triaxial stress state was investigated in [120] using a standard Hoek's cell. The results proved that the presence of constant radial horizontal stresses increases the vertical compressive strength up to $3f_b$, with respect to uniaxial tests. Instead, a smaller increase in strength occurs if increasing radial stresses are applied with a constant vertical loading. In the same study, the biaxial strength of AAC was found to be approximately equal to $1.1f_b$.

Finally, AAC compressive strength depends on the moisture content of the samples at the time of testing; for this reason, tests should be performed on specimens in an equilibrium condition with the surrounding environment [16,39,113]. According to the variability range suggested in [62], a reduction in the moisture content is associated with an increase in compressive strength, up to a maximum value corresponding to the dry state. This aspect is also dealt with in most of the standards ruling compressive tests. For example, the European standard [87] allows different conditioning methods for specimens, that is, conditioning to the air dry condition, to the oven dry condition, to $6 \pm 2\%$ moisture content, or by immersion. In case of conditioning to dry air condition and conditioning to $6 \pm 2\%$ moisture content, the experimental values of compressive strength can be accepted as they are. Otherwise, if specimens are subjected to conditioning to the oven dry condition or by immersion, a correction factor should be applied to experimental results (respectively equal to 0.8 and 1.2, according to [87]). When specimen conditioning requires a thermal treatment in the oven (which is generally allowed for every type of conditioning, except for immersion), particular attention should be paid to the maximum applied temperature, because a faster heating is often associated with the formation of smeared shrinkage cracks, hence potentially weakening the specimen.

3.4. Modulus of rupture, splitting tensile strength and fracture energy

Tensile behavior of AAC can be characterized through flexural [92] or splitting tests, as alternative to the execution of direct tensile tests. Tensile strength can be also derived by tensile tests according to EN 1607 [121] and EN 1608 [122]. Tensile strength is obviously dependent on material density ρ, but most of the relations available in the literature allow prediction of tensile strength as a function of compressive strength. Among several motivations, those relations rely upon a satisfactory statistical dependence of tensile strength upon its compressive counterpart, the latter being also considered the most important mechanical property in case of geomaterials such as concrete and masonry. This means that tensile strength is thus associated with another mechanical property that is expected to be known or assumed in most cases.

Although EN 771-4 [47] does not report any relationship between flexural strength and compressive strength, the standard for prefabricated reinforced components on AAC (EN 12602 [86]) provides the following relationship in terms of characteristics values:

$$\begin{aligned} f_{t,flk;0.05} &= 0.18\, f_{ck} \\ f_{t,flk;0.95} &= 0.36\, f_{ck} \end{aligned} \quad (1)$$

where f_{ck} is determined according to EN 679 [123].

One of the best known relationships between flexural tensile strength $f_{t,fl}$ (so called modulus of rupture, MOR) and compressive strength f_b is that suggested by RILEM recommendations [62] as follows:

$$f_{t,fl} = 0.27 + 0.21\, f_b. \quad (2)$$

Other relationships calibrated on experimental data (coming from specific experimental programs) can be found in the literature [52,107,116]. However, for a given compressive strength value, the corresponding predictions of MOR appear to be quite different from each other (see, for example, the comparison reported in [16]). The trend of variation of MOR with moisture is found to be similar, even if not identical, to that of compressive strength [16,62]. Flexural tensile strength is higher than direct tensile strength f_t, reaching 0.2–0.4 of compressive strength f_b [7,13,39,62].

According to [62], splitting tensile strength $f_{t,spl}$ is around 50% of direct tensile strength f_t and tends to decrease slightly as the moisture content increases. ACI 523.4R-09 [124] suggests a proportionality factor of 0.5 between splitting $f_{t,spl}$ and flexural tensile strength $f_{t,fl}$, based on the analysis of the experimental data reported in [107,116]. A linear relationship between $f_{t,spl}$ and f_b is suggested by the Dutch Standard NEN 3838 [125]:

$$f_{t,spl} = 0.08125\, f_b. \quad (3)$$

The knowledge of tensile behavior requires also the determination of fracture energy, which can be intended as an indicator of the fracture toughness of the material [62,126]. Fracture energy G_F can be obtained experimentally by either wedge-splitting tests or three-point bending tests on notched specimens (see Fig. 6a) [114,127–129], which allow plotting the complete load–crack opening displacement curve and deriving the cohesive law for the material (Fig. 6b).

According to [126], G_F is influenced by the grain size of the silica fraction in the admixture (being higher in case of coarser quartz), the duration of the autoclaving process, and material density. An almost linear relationship between G_F (in N/m) and ρ (in kg/m^3) can be derived from the experimental data recently reported in [16,130]:

$$G_F = 0.0135\, \rho - 1.83. \quad (4)$$

G_F is also influenced by specimen geometry, increasing for higher values of fracture ligament length and specimen thickness [128]. Furthermore, G_F is higher (while tensile strength is lower) when measured parallel to the direction of rising. The influence of moisture content on fracture parameters seems instead very limited [16,128,131]. Based on experimental results available in the literature, it can be inferred that AAC is a softening material and therefore the fictitious crack model can be successfully applied to describe the cracking process. Accordingly, the dominant parameter for the description of fracture behavior in AAC structural members is the characteristic length, which can be defined as follows:

$$l_{ch} = \frac{E_c \cdot G_F}{f_t^2} \quad (5)$$

where E_c is the secant modulus of elasticity, G_F is the fracture energy and f_t is the direct tensile strength. Given the same size, structural members with higher values of l_{ch} are able to better withstand cracking [62,128].

3.5. Elastic parameters

Fig. 7 shows the range of variation for the modulus of elasticity as a function of ρ for AAC blocks tested according to the European standard EN 1352 [90] for the blue marks and according to the Chinese standard

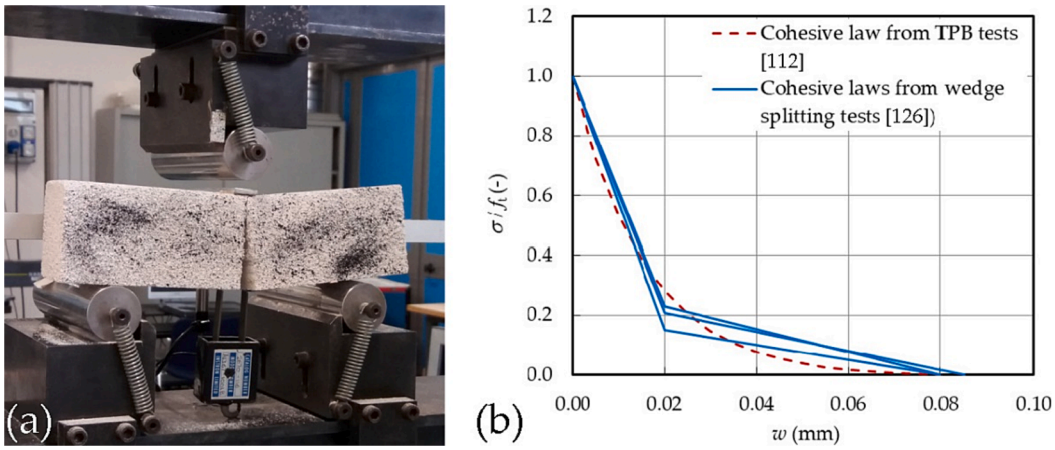

Fig. 6. (a) Three-point bending (TPB) tests on a notched specimen for determination of G_F; (b) comparison between cohesive laws derived from wedge splitting tests and TPB tests for AAC with ρ ranging from 400 to 550 kg/m^3 (adapted from [114]).

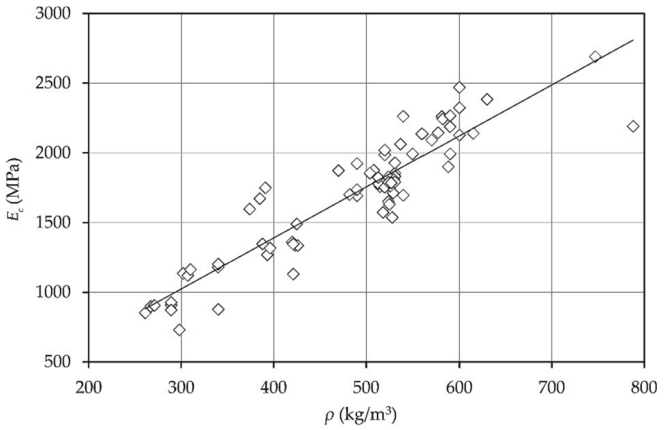

Fig. 7. Range of variation of modulus of elasticity vs. dry density of AAC blocks [blue marks: Xella Technologie- und Forschungsgesellschaft mbH, red marks: Chen et al. [106]]. (For interpretation of the references to colour in this figure legend, the reader is referred to the web version of this article.)

GB/T 17431.2-2010 [132] for the red marks.

The EN 12602 Standard [86] reports the following equation:

$E_c = 5(\rho - 150) \quad (\rho \text{ in } kg/m^3)$. (6)

The dependency of E_c on ρ is almost linear also according to [62], as follows:

$$E_c = (-520 + 4.7\rho) \pm 500\ MPa. \tag{7}$$

However, most of the equations reported in the literature correlate the modulus of elasticity to the compressive strength measured on cubes or prisms [39,52,107,116], or in some cases to both ρ and compressive strength [13,39]. Some of the abovementioned equations are reported in the following for reading convenience:

$$E_c = 1550\, f_b^{0.7} \quad (f_b \text{ in } kg/cm^2); \tag{8}$$

$$E_c = 3000\, f_{cp} \quad (f_{cp} \text{ in } kg/cm^2); \tag{9}$$

$$E_c = 6500\, f_{c,cores}^{0.6} \quad (f_{c,cores} \text{ in } psi); \tag{10}$$

$$E_c = 0.3\, f_{c,cores} + 105 \quad (f_{c,cores} \text{ in } psi); \tag{11}$$

$$E_c = 6000\, \rho^{1.5} f_b \quad (\rho \text{ in g/cm}^3, f_b \text{ in } kg/cm^2); \tag{12}$$

$$E_c = k^*\, \rho\, f_b^{0.5} \quad (\rho \text{ in } kg/m^3, f_b \text{ in MPa}, k^* = 1.5 - 2) \tag{13}$$

The elastic modulus decreases under increasing moisture content [62], while it increases with increasing loading speed during the test [117]. The value of the modulus of elasticity is also influenced by the mixture composition. In the case of cellular concretes containing pozzolanic materials, E_c varies considerably according to the nature of the pozzolan itself, even under the same density and compressive strength [13].

Poisson's ratio is almost constant and equal to about 1/6, regardless of density and compressive strength. For practical applications, an approximate value of 0.2 is recommended in [62].

3.6. Shrinkage

The high porosity, together with the specific surface of pores (around 30–50 m^2/g), make AAC highly prone to shrinkage [39,133]. This tendency is even more accentuated by the lack of coarse aggregates in the admixture [40]. Shrinkage is reported to increase with a decrease in pore size (or with an increase in the amount of smaller pores; see, e.g., [39,134,135]), and it is also affected by pore distribution [136]. Other factors affecting shrinkage and basically related to the production process are the type of binder (cement, lime or a mixture of them), the type of aggregate (with the possible replacement of sand with other silica sources, like for example fly ash), as well as autoclaving conditions [133,136,137]. On this last point, it can be noted that a higher degree of crystallization of calcium silicate hydrate phases in the final products improves the characteristics of AAC blocks, reducing their tendency to shrinkage [40,108]. It was found that shrinkage is instead almost independent of the dosage of aerating agent, silica fume and superplasticizer [133].

Time evolution of the measured shrinkage is also controlled by extrinsic factors, such as the specimen size and the relative humidity of the environment [62]. Shrinkage increases in case of larger cross sections, and with a decrease in relative humidity, according to [136]. Drying process is obviously faster in case of elevated temperatures [62]. Finally, shrinkage is related to the moisture content of the element at the beginning of the drying process: the higher the moisture content, the higher the shrinkage. Only in case of moisture contents greater than 20% by volume, the loss of moisture causes a relatively small shrinkage [136]. Final shrinkage strain can be roughly estimated as the product between the variation of humidity (in percentage) and the coefficient of linear hygral dilatation, which can be assumed equal to $0.9 \cdot 10^{-5}\ \%^{-1}$ for AAC.

3.7. Thermal conductivity

Among functional properties, thermal conductivity λ of AAC is drawing an ever-increasing attention from manufactures due to its influence on the amount of heat losses through external walls, which in turn affects energy consumption in buildings. The λ-values of AAC can be up to 10 times lower with respect to normal concrete, and they usually range from 0.07 to 0.2 *W/(mK)* in a ρ interval between 300 and 750 kg/m^3 [138–142].

Thermal conductivity is mainly influenced by raw materials used in the production process, moisture content, and above all, density [39]. Based on literature data, a good correlation between λ in the dry state and ρ has been found in the range 300–600 kg/m^3 (Fig. 8). This finding may be an indication that producers have reached their current limits in the homogenization of pore structure within their AAC products [139–141]. The amount of pores and their distribution is indeed critical for λ [39,42]. Although it is clear that thermal performances can be improved by reducing the material density (due to the corresponding increase in porosity), it should be underlined that finer pores guarantee a better thermal insulation as well [39,143].

The variation of λ-values over different dry densities and moisture contents calculated according to EN 1745 [98] and EN ISO 10456 [145] is reported in Fig. 9, according to Schoch and Kreft [146]. On the other hand, some studies report that the value of λ increases under increasing moisture content [147,148], up to a critical value around 15% [149]. Jin et al. [149] found indeed that below this critical value, λ increases more significantly than in case of higher moisture content levels. According to [140], the increase in thermal conductivity of AAC may be up to six times passing from the dry state to capillary water saturation condition. However, this behavior is mainly influenced by the wall thickness and weather conditions.

Since λ-values included in various standards and technical sheets from manufacturers are referred to the dry state only (so-called $\lambda_{10,dry}$, according to [150]), a design value λ_d is used in engineering practice. To that aim, a correction factor is therefore introduced to take into account moisture influence [39,62]. Moisture conversion factors are usually specified in national regulations. However, Schoch and Kreft [146] compared the measurements with the calculations done according to the European standards EN ISO 10456 [145] and EN 1745 [98], by assuming a dry density equal to 400 kg/m^3 and the calculation value of heat conductivity $\lambda_R = 0.10$ *W/mK*. The measurements according to DIN 52612 [151] show a considerably lower additive allowance and no exponential increase in dependence of moisture than the calculation (Fig. 10).

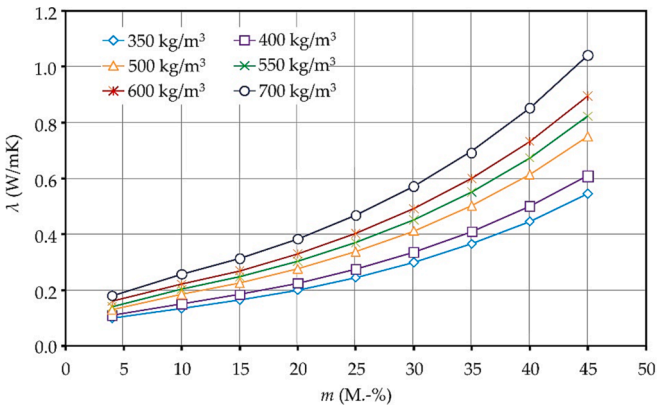

Fig. 9. Relationship between calculated λ-values over different dry densities ρ and moisture contents *m* between 4 M.-% and 45 M.-% according to EN ISO 10456 [145] using the fixed moisture correction coefficient $f_u = 4$ according EN 1745 [98] (adapted from [146]).

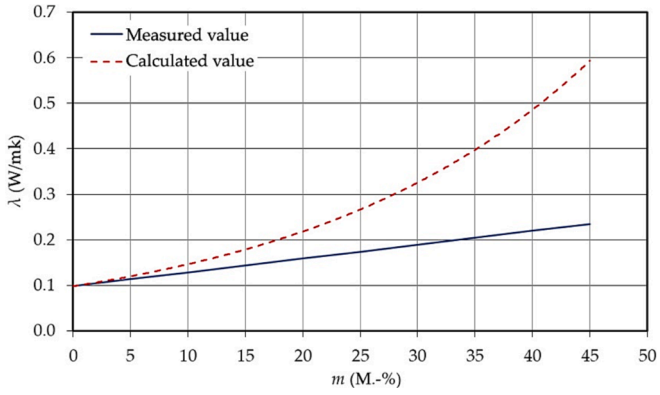

Fig. 10. Dependence of λ-values on moisture contents. Measured vs. calculated data according to European regulations (EN ISO 10456 [145], EN 1745 [98], red line). (For interpretation of the references to colour in this figure legend, the reader is referred to the web version of this article.)

Other relations between λ and *m* can be found in [147,152,153], but a general agreement on this point has not been reached yet. The dependence of λ on temperature is reported to be far less important than its dependence on moisture. According to Jerman et al. [140] in the

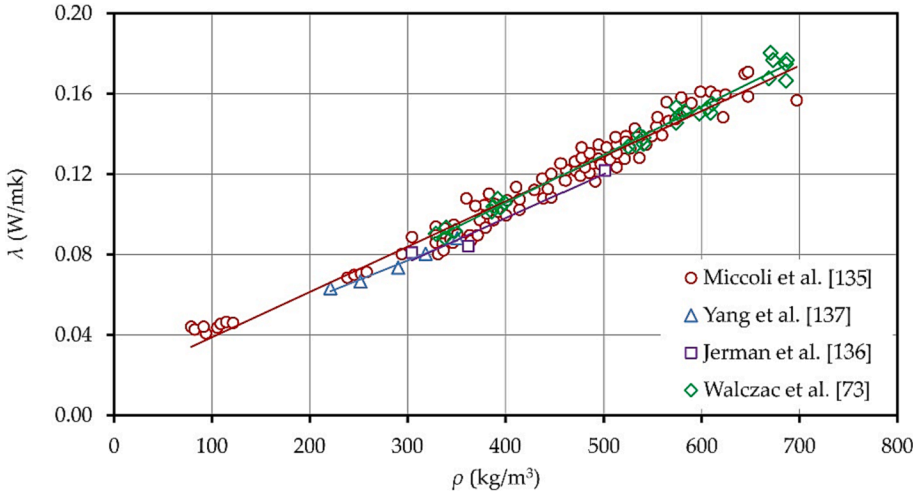

Fig. 8. Relationship between measured λ and ρ (adapted from [16]). Values of thermal conductivity were calculated according to EN 1745 [98] for data by Miccoli et al. [139] and Jerman et al. [140] and EN ISO 6946 [144] for data by Walczac et al. [74].

temperature range 2–40 °C the increase of λ was up to 50% only.

As regards raw materials, it has been observed that thermal conductivity can be reduced by reducing the amount of residual quartz in the final product. Such an outcome can be achieved without changing the production process but simply through the use of finer ground quartz and the adaptation of the binder content [142]. Given the same porosity and ρ, the thermal conductivity of sand based and fly ash based AAC is reported to be 8.3% higher than that of fly ash aeration AAC [40,143]. Replacement of ingredients with substances with low specific gravity, such as rice husk ash, coal bottom ash, zeolite, or perlite waste [22], can lead to a reduction of λ ranging between 30% and 50% [63,76,154]. Finally, it has been pointed out that autoclaving conditions play a minor role on this property [39,40].

4. Mortar for AAC masonry

4.1. Standards for material testing

The mortar, designed for assembling of masonry of AAC units with thin-layer mortar joints of 1 *mm*, must follow the recommendations by EN 998-2 [155]. Material tests on thin-layer mortars must be performed to characterize uniaxial compressive strength (EN 1015-11 [156]), flexural strength (EN 1015-11 [156]), dry bulk density (EN 1015-10 [157]), bulk density of fresh mortar (EN 1015-6 [158]), and slump (EN 1015-3 [159]).

4.2. Mortar requirements

AAC masonry is made by assembling the blocks using mortar, usually thin layer mortar (TLM) in Europe, while general purpose mortar (GPM) and polyurethane foam can be found in Extra-EU countries and in some research works.

The TLM mortar is composed of white or grey cement (exceptionally sulphate-resistant hydraulic binder), siliceous sand, water retention admixture (such as cellulose), additives to improve workability and setting time, and polymers for a good adhesion to the block. Mortar is provided in dry ready-mixed bags that require just the addition of water (6–7 *L* per 25 *kg*) with a prescribed mixing sequence. The special composition of mortars allows avoiding pre-wetting of the blocks in ordinary environmental conditions. M5 mortar, or more frequently M10 mortar, is used so that its mechanical properties are compatible with those of the blocks. Typical lower-bound values of compressive and flexural tensile strengths are 10 *MPa* and 3 *MPa*, respectively. A summary of the typical properties of mortar commercialized in Europe is reported in Table 1. The limits for the mortar properties are reported in EN 998-2 [155].

Properties of mortars used in the U.S.A. are slightly different. For instance, in that country, mortar may be applied in thin beds (1.6-*mm* thick) or thick beds (9.5-*mm* thick) with a compressive strength ranging from 13.8 to 34.5 *MPa* [162]. In India and China, the use of general purpose mortar (GPM) and thick bed joints (approximately 10-*mm* thick) is more common. In this case, it is advisable to pre-wet the blocks. Furthermore, because the mortar-block adhesion is generally limited, some authors propose to coat the blocks with cement slurry.

Sometimes, a single-component, low-expanding, polyurethane (PU) foam is used for thin-layer application, usually applied in the form of stripes. This foam is employed also to seal the joints between AAC walls and the surrounding structure (typically concrete or steel) in framed buildings. However, the material behavior is very different when used as a mortar substitute or for joints sealing. In the latter case, swelling materials are used. In the mortar joint, the PU foam should be dimensionally stable. Usually, the use of PU foam is limited to internal and non-loadbearing walls that do not require fire resistance.

Table 1
Typical values of physical and mechanical properties of TLM commercialized in Europe.

Mortar property	Value/Range/ Class	Reference for testing
Maximum grain size (*mm*)	0.6–2	EN 1015-1 [160]
Bulk density of hardened mortar (kg/m^3)	1300–1600	EN 1015-10 [157]
Water per 25 *kg* of dry mortar (*l*)	5.75–7.5	
Consistence of fresh mortar (*mm*)	17.5 ± 1 mm	EN 1015-3 [159]
Minimum thickness (*mm*)	0.5	
Maximum thickness (*mm*)	0.5–3	
Compressive strength after 28 days (*MPa*)	5–15	EN 1015-11 [156]
Adhesive strength of hardened mortar on substrates (*MPa*)	> 1.0	EN 1015-12 [94]
Initial shear strength (*MPa*)	> 0.3	EN 1052-3 [95]
Reaction to fire	A1	EN 13501-1 [161]
Thermal conductivity (*W/mK*)	0.39–0.67	EN 1745 [98]
Flexural strength after 28 days (*MPa*)	> 3	EN 1015-11 [156]

5. Mechanical characterization of AAC masonry assemblages

Several studies can be found in the literature on the mechanical behavior of AAC masonry. Those studies mainly deal with compressive, shear, and flexural response under static or cyclic actions. The present work focuses on the static behavior. Experimental tests are usually carried out on masonry walls or smaller assemblages formed by blocks and mortar (wallets, triplets, etc.), while there have been so far only limited studies on the behavior of wall joints, although the latter are subjected to huge levels of stress concentration and cracking [163]. However, these studies are certainly noteworthy because EN 1996-1-1 [164] requires checking of the connections between shear walls and flanges of intersecting walls against vertical shear.

Besides the review of literature results, an overview of the European standards currently used to determine the main structural properties of AAC masonry with thin-layer mortar and filled vertical joints is also provided.

5.1. Behavior in compression

5.1.1. Standards for determination of the compressive strength of AAC masonry

Masonry compressive strength has to be experimentally characterized according to EN 1052-1 [165]. Such a European standard establishes that the characteristic compressive strength f_k is the minimum strength estimate of specimens out of the mean value divided by 1.2 and the lowest single value of the measured ultimate stresses:

$$f_k = \min\left\{\frac{f_{mean}}{1.2}; f_{i,min}\right\} \tag{14}$$

If five or more specimens are tested, f_k is assumed to be the 5% fractile calculated from the whole data set. As alternative, f_k can be calculated according to Equation (15) as per EN 1996-1-1 [164]:

$$f_k = K f_b^{\alpha} \tag{15}$$

where $K = 0.80$ and $\alpha = 0.85$ for AAC masonry with thin-layer mortar according to Table 3.3 of EN 1996-1-1 [164]. As reported by Drobiec et al. [166], the National Annexes adopt different values of K and α into Equation (15). Concerning the AAC masonry with thin-layer mortar, the German National Annex in Table NA.10 uses $K = 0.90$ and $\alpha = 0.75$. In the Belgian National Annex, the values of coefficients are $K = 0.80$ and $\alpha = 0.85$. Finally, in the Finnish National Annex, such coefficients are set to $K = 0.85$ and $\alpha = 0.85$.

The modulus of elasticity E can be calculated as secant modulus from the stress σ at one-third of f_i according to EN 1052-1 [165], which approximates the stress under service load. The respective strain ε_i is the mean value of four measurements in the load direction:

$$E_i = \frac{f_i}{3\,\varepsilon_i} \tag{16}$$

In addition, EN 1996-1-1 [164] proposes the following equation to estimate the value of E:

$$E = K_E f_k \tag{17}$$

where K_E is a constant defined by National Annexes. Among them, the German National Annex DIN EN 1996-1-1NA [167] proposes a value of $K_E = 550$ for AAC masonry with thin-layer mortar.

5.1.2. Literature survey: Characterization of AAC masonry in compression

To characterize masonry assemblages in compression, tests are usually performed on masonry wallettes [165], or stack-bond-bricks [168].

Daou [169] studied the influence of unit strength, mortar strength, and size of the units on the compressive strength of AAC wallettes made with GPM. The author observed that the strength of the wallettes is affected by the strength of the blocks, while the strength of the mortar has less importance.

Drobiec et al. [112,166] studied the influence of the type of mortar on the compressive behaviour of AAC wallettes using AAC units with $f_b = 4.0$ *MPa*. In detail, those researchers compared the behavior of wallettes assembled with no mortar, TLM, polyurethane foam, and GPM. Furthermore, they investigated the case of filled/unfilled vertical joints and the use of two strips/complete mortar layer. The experimental results showed a cracking stress f_{cr} equal to about 80–90% of compressive strength, with a variation of 20% depending on the type of mortar joint. In case of TLM, unfilled vertical joints (UVJ) allowed a higher compressive strength to be obtained, reducing the modulus of elasticity. The polyurethane foam provided higher strength, but deformability was approximately three times the one of TLM with filled vertical joints (FVJ) (see Table 2).

Ferretti et al. [170] tested square masonry wallettes built with small size units with $f_b = 3.1$ *MPa* (250 × 50 × 100 mm^3), TLM, and FVJ. A compressive load with different angles (0, 22°, 45°, 68°, 90°) with respect to the normal to the bed joints was applied (Fig. 11a). Results showed that the crack pattern varies with the angle of the applied load, with a transition from vertical cracks through the blocks to sliding cracks in the mortar joints. The compressive strength f_{mean} has a slight variation, from 2.1 to 2.6 *MPa*, probably because the type of mortar provides a substantially isotropic behavior to masonry. The same researchers performed the tests also with a biaxial state of stress. In this case, the wallettes suffered cracks through the wallette thickness and the strength was similar to that measured with vertical forces.

The characterization of AAC walls in compression by means of non-destructive techniques based on the acoustoelastic (AE) method was recently proposed in [171,172]. Such a technique can be succesfully applied to AAC because of its high homogeneity due to its industrial production, allowing an accurate evaluation of the average stresses in the walls if a sufficiently large number of measurement points is selected.

Frequently, AAC walls are reinforced in the bed joints to improve their shear resistance under seismic actions. The effect of steel trusses, fibreglass geogrids, and basalt fiber reinforced polymer (FRP) meshes were discussed in [173–175]. Experimental data are summarized in Table 3, AAC units with $f_b = 4$ *MPa* were used. Although the influence of bed-joint reinforcement on compressive strength of the masonry is limited, the reinfocerment contributes mostly to increase the in-plane and out-of-plane resistance. A slight increase in cracking, compressive stress f_{cr} and modulus of elasticity E was observed in case of basalt FRP mesh and UVJ.

Table 2
Results of compression tests on AAC masonry wallettes with different types of mortar [166].

Series	f_{cr} (*MPa*)	f_{mean} (*MPa*)	E (*MPa*)	ν (–)
S0N without mortar	2.61	3.15	564	0.11
S1N TLM, UVJ	2.35	2.97	2040	0.18
S2N TLM, FVJ	2.08	2.61	2447	0.18
S3N GPM, UVJ	2.30	2.52	2279	0.15
S4N thin-layer strip mortar, UVJ	2.04	2.31	2379	0.18
S5N polyurethane foam, UVJ	2.52	3.00	770	0.23
S6N GPM, FVJ	2.19	2.74	2401	0.18

5.2. Flexural behavior

5.2.1. Standards for determination of the flexural strength of AAC masonry

Flexural strength can be calculated according to EN 1052-2 [176] using the following equation:

$$f_{xi} = \frac{3\, F_{max,i}\, (l_1 - l_2)}{2\, b\, t_u^2} \tag{18}$$

If the test sample consists of five specimens, the characteristic value of flexural strength can be estimated as follows:

$$f_{xk} = \frac{f_{x,mean}}{1.5} \tag{19}$$

In case of more than five specimens, f_{xk} has to be calculated by statistical processing of the whole experimental data set as follows:

$$f_{xk} = 10^{y_c} \tag{20}$$

$$y_c = y_{mean} - k\, s \tag{21}$$

where s is accounted for n logarithmic strength values y_i (i.e. $y_i = \log_{10} f_{xi}$). Characteristic values of flexural strength f_{xk1} and f_{xk2} are given by EN 1996-1-1 [164] and can be calculated according to Section 3.6.4, Note 3 [164], where $f_{xk1} = 0.035\, f_b$ and $f_{xk2} = 0.035\, f_b$ (for filled vertical joints). Alternatively, the characteristic flexural strength values can be assumed according to tables in Section 3.6.4, Note 3 [164], where for TLM $f_{xk1} = 0.15$ *MPa* and f_{xk2} is equal to 0.20 *MPa* ($\rho < 400$ *kg/m*^{3}) and 0.30 *MPa* ($\rho \geq 400$ *kg/m*^{3}).

5.2.2. Literature survey: Characterization of AAC masonry in bending

Flexural tests to study the out-of-plane behaviour of masonry are usually performed on rectangular panels assembled using at least four courses of blocks, following EN1052-2 standard [176].

Piekarczyk [177] tested panels assembled with AAC blocks ($f_b = 4.04$ *MPa*, with a mortar having a mean compressive strength of 6 *MPa*), measuring a flexural strength of 0.11 *MPa*. Adding reinforcement in the bed joints (i.e. steel trusses, glass nets, or basalt nets) produced an increase in flexural strength up to 0.26 *MPa*. Ahmed and Fried [178] tested low-density brickworks (with $f_b = 2$–2.8 *MPa*) obtaining a flexural strength varying from 0.16 to 0.48 *MPa* depending on block type, mortar (TLM, and GPM), and direction of the plane of failure (parallel or perpendicular to the bed joints). Al-Shaleh et al. [179] compared the flexural behaviour of non-loadbearing masonry walls made of AAC blocks. Similarly to [170], those researchers found that the flexural strength of AAC wallettes constructed with epoxy glue mortar is similar for bending parallel (0.27 *MPa*) or perpendicular (0.32 *MPa*) to the bed joints. Shaleh et al. also observed that the flexural strength increases with the block thickness under a given block length.

Ferretti et al. [170] tested in-plane flexural behaviour of AAC masonry panels assembled with small-size blocks ($\rho = 550$ *kg/m*^{3}, $f_b = 3.1$ *MPa*) and M5 TLM (with mean compressive strength of 6 *MPa*, and mean flexural strength of 2.7 *MPa*), as shown in Fig. 11b. For bed joints placed horizontally and vertically, those researchers measured flexural strengths of 0.37 *MPa* and 0.30 *MPa*, respectively. The corresponding values of fracture energy G_F were 7.1 *N/m* and 5.15 *N/m*. In both cases, flexural cracks started in the masonry joints. Experimental results are very close to that determined on specimens with the same geometry but entirely made of AAC, with a mean value of G_F equal to 6.2 *N/m*.

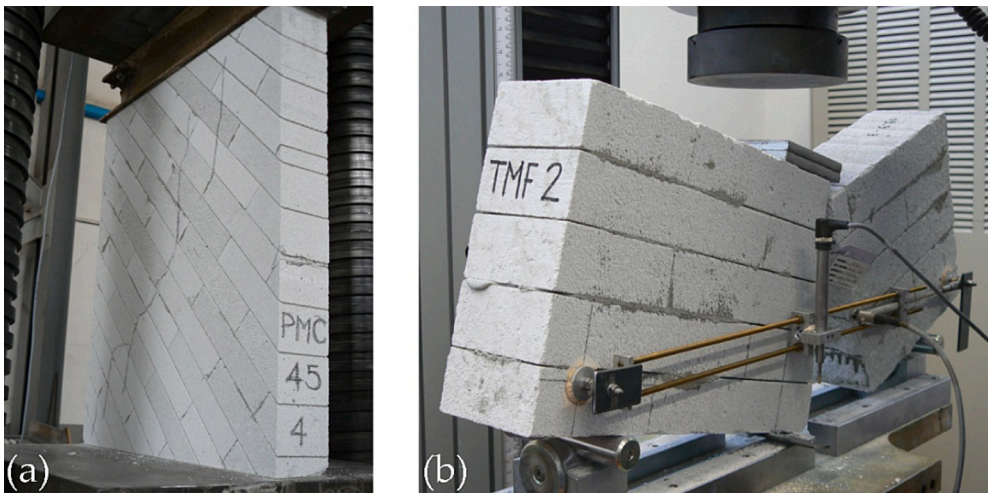

Fig. 11. (a) Compression test on masonry wallettes with inclined joints; (b) three-point-bending tests to investigate in-plane behavior of AAC masonry.

Table 3
Results of compression tests on AAC masonry wallettes with different types of reinforcement [173,174].

Series	f_{cr} (*MPa*)	f_{mean} (*MPa*)	E (*MPa*)	ν (–)
S1N unreinforced, UVJ	2.35	2.97	2040	0.18
S2N unreinforced, FVJ	2.08	2.61	2447	0.18
S1Zk truss, UVJ	2.85	3.12	2363	0.26
S1ZSt synthetic mesh, UVJ	2.59	3.03	1753	0.22
S1ZSb basalt mesh, UVJ	2.98	3.52	2484	0.33
S2Zk truss, FVJ	2.48	2.84	2213	0.21
S2Zst synthetic mesh, FVJ	2.65	2.99	2401	0.17
S2ZSb basalt mesh, FVJ	2.51	2.83	2358	0.25

5.3. Shear behavior

5.3.1. Standards for determination of the shear strength of AAC masonry

Shear strength of AAC masonry can be tested as suggested by EN 1052-3 [95]. The values of f_{v0i} and f_{pi} are evaluated by means of the following relationships:

$$f_{v0i} = \frac{F_{max,i}}{2A_i} \tag{22}$$

$$f_{pi} = \frac{F_{pi}}{A_i}. \tag{23}$$

According to Section 3.6.2 of EN 1996-1-1 [164], the value of f_{vk0} is then determined from the results of tests on masonry using a reduction factor equal to 0.8. The value of f_{vk} is defined using thin-layer mortar in beds with thickness ranging from 0.5 to 3.0 *mm*, in accordance with Clause 3.2.2 of EN 1996-1-1 [164] with all joints satisfying the requirements in Section 8.1.5 of EN 1996-1-1 [164], so as to be considered as filled. Hence, f_{vk} may be estimated through Equation (24) but should not be greater than $0.065 f_b$ or f_{vlt}:

$$f_{vk} = f_{vk0} + 0.4\,\sigma_d \tag{24}$$

where σ_d is perpendicular to the shear in the member at the level under consideration, using the appropriate load combination based on the average vertical stress over the compressed part of the wall that is providing shear resistance. The f_b-value is considered in the direction of loading on the test specimens being perpendicular to the bed face, as described in Section 3.1.2 of EN 1996-1-1 [164]. Consequently, for AAC masonry f_{vk0} may be determined from the values given in Table 3.4 of EN 1996-1-1 [164], where a value of 0.30 *MPa* is declared when thin-layer mortar is used.

However, the German National Annex of EN 1996-1-1 includes an additional relationship to assess the shear behavior considering the tensile failure of the unit, as follows:

$$f_{vlt} = 0.45\, f_{bt,cal} \sqrt{1 + \frac{\sigma_d}{f_{bt,cal}}} \tag{25}$$

$$f_{bt,cal} = \frac{0.082}{1.25} \cdot \frac{1}{0.7 + \left(\frac{f_{st}}{25}\right)^{0.5}} f_{st} \tag{26}$$

where f_{st} is the converted value of the compressive strength class of the AAC units [24] multiplied by 1.25.

5.3.2. Literature survey: Characterization of AAC masonry in shear

5.3.2.1. Tests on triplets. Shear strength of AAC masonry is usually measured on triplets (Fig. 12a) according to EN 1052-3 [95]. Other shear testing procedures for masonry are those performed on either couplets (i.e. couplet shear tests) or double-layer masonry specimens (i.e. direct shear tests), with different pros and cons discussed in [180]. In all these types of shear test, masonry strength is characterized with respect to shear sliding failure along single mortar joints. Otherwise, shear strength may be characterized with respect to diagonal shear failure, which may be associated with either a stair-stepped crack pattern involving both head and bed joints (diagonal shear sliding failure), or diagonal crack pattern passing through masonry units (diagonal tension failure). Therefore, diagonal shear strength is associated with another testing procedure discussed in Sect. 5.3.2.2, which – even in case of regular masonry assemblage – deals with a composite resisting mechanism that does not involve only shear sliding strength of bed joints but also tensile strength of head joints and/or tensile strength of masonry units.

Regarding triplet testing, Rosti et al. [181] measured the shear strength of low-density AAC units ($\rho = 360\ kg/m^3$, $f_b = 3.06$ MPa) and TLM with three values of confining stress orthogonal to the bed joints (0.1, 0.2, and 0.3 *MPa*). Results provided initial shear strength $f_{v0} = 0.29$ *MPa* and friction coefficient $\mu = 0.5$. The same tests under zero confining stress provided a larger strength ($f_{v0} = 0.32$ *MPa*), probably because of the rotation of the blocks related to the test setup. This is a drawback that can be completely solved through direct shear testing, which was successfully performed on several masonry assemblages (see e.g. [182,183]). Jasinki and Drobiec [174] performed triplet shear tests on normal-density AAC units ($\rho = 600\ kg/m^3$, $f_b = 4.0$ *MPa*), M5 TLM, and confining stress equal to 0.1, 0.3, and 0.5 *MPa*. Those researchers obtained $f_{v0} = 0.31$ *MPa* and $\mu = 0.62$. For a similar value of material density and TLM, Bhosale et al. [184] obtained a shear strength $f_{v0} = 0.22$ *MPa* from tests with zero compressive stress. In all three

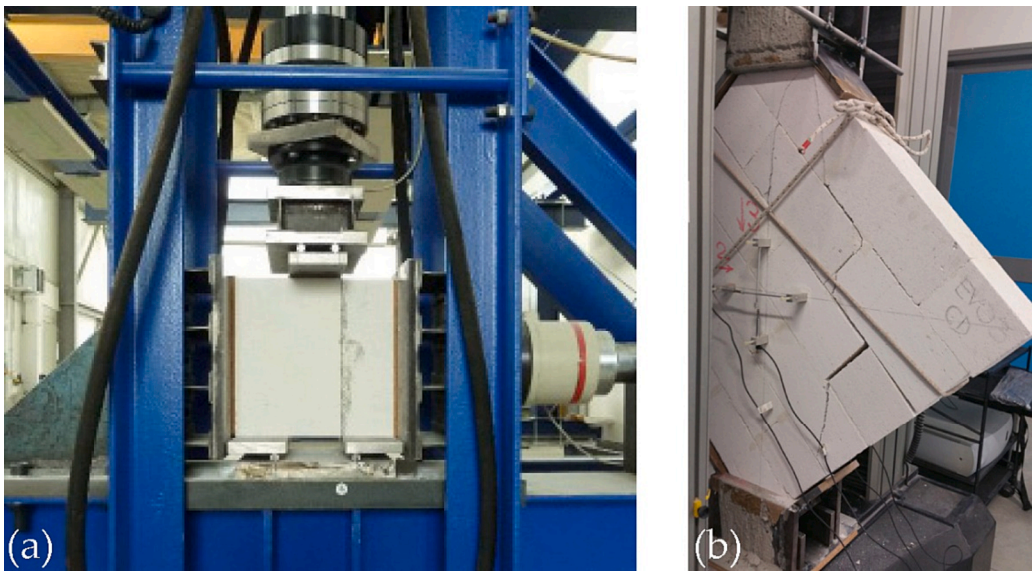

Fig. 12. (a) Shear test on triplet [source: Xella Technologie- und Forschungsgesellschaft mbH]; (b) diagonal compression test.

Table 4
Results of compression tests on AAC masonry wallettes with different types of reinforcement [174,181,190].

Author	$t_u \times l \times h$ (mm^3)	f_b (*MPa*)	f_{mortar} (*MPa*)	ρ (kg/m^3)	τ (*MPa*)	f_{mean} (*MPa*)	G (*MPa*)	*Notes*
Rosti el al. [181]	300 × 1000 × 1000	3.06	15.75	360	0.23	1.91	357	
Kubica & Galman [190]	240 × 900 × 805	4.65	12.4	600	0.20	4.65	357	UVJ
Jasinsky & Drobiec [174]	180 × 1180 × 1212	4.0	6.1	600	0.196	2.97	329	UVJ
Jasinsky & Drobiec [174]	180 × 1180 × 1212	4.0	6.1	600	0.292	2.62	561	FVJ
Jasinsky & Drobiec [174]	180 × 1180 × 1212	4.0	11.9	600	0.189	–	363	UVJ

experimental programs described in [174,181,184], the measured values of shear sliding strength under zero confining stress are smaller than the nominal shear strength $f_{vk0} = 0.3$ *MPa* reported in EC6 [164], regardless of mortar or block strengths. On the contrary, the friction coefficient provided by EC6 (i.e. $\mu = 0.4$) is smaller than its experimental estimates.

Raj et al. [185] investigated the influence of mortar type on shear strength of assemblages realized with AAC blocks with ρ between 569 and 684 kg/m^3, and $f_b = 2.07$ MPa. Tests were performed on triplets without confining stress. Results showed that, in case of GPM, the bond strength of AAC masonry increased with cement content in the mortar, while remaining smaller than 0.07 *MPa*. Shear strength increased by applying a cement slurry coating to the units (0.25 *MPa*) or by using thin-layer polymer modified mortar (0.19 *MPa*). Jasinski el al. [174] investigated the influence of mortar on shear strength, considering not only M5 TLM ($f_{v0} = 0.31$ *MPa*, $\mu = 0.62$), but also two strips of M5 TLM ($f_{v0} = 0.13$ *MPa*, $\mu = 0.67$), and two strips of polyurethane glue ($f_{v0} = 0.28$ *MPa*, $\mu = 0.53$). Schmidt et al. [186] studied GPM triplets with confining stress (0.1, 0.2, and 0.3 *MPa*) obtaining $f_{v0} = 0.08$ *MPa*. Adopting DIN 18555-5 [187] instead of EN 1052-3 [95] standard, the initial shear strength was nearly double ($f_{v0} = 0.15$ *MPa*). However, DIN 18555-5 [187], which is usually adopted for calcium-silicate units, takes into account smaller specimens than those adopted by EN 1052-3 [95]. Finally, Vanheukelhom et al. [188] investigated the effect of damp-proof courses on the initial shear strength.

5.3.2.2. Diagonal compression tests. As alternative of the method presented in the previous section, shear strength of masonry can be calculated through the assessment of the diagonal shear failure [37]. For this reason, some researchers suggest to perform also diagonal compression tests on AAC masonry specimens according to ASTM E-519-2 [189]. In diagonal compression tests, bed joints are inclined at approximately 45° with respect to the vertical load direction and failure occurs with either diagonal cracks or stepwise cracks, as shown in Fig. 12b (especially in case of unfilled head joints). Some results reported in the literature are summarized in Table 4. The shear strength τ is moderately influenced by the mortar compressive strength (from 0.23 to 0.29 *MPa*), increasing from 0.196 to 0.292 *MPa* in the case of filled head joints. Jasinski and Drobiec [174] observed that the installation of a reinforcement in the bed joints, embedded within two layers of mortar, permitted an increase in diagonal shear strength from 0.196 to 0.269 *MPa* and 0.242 *MPa* in case of steel mesh and fibreglass geogrid, respectively.

6. Conclusions

In this paper, the physical properties and mechanical behavior of AAC masonry, as well as empirical relationships/models, standard provisions, experimental data and testing procedures, have been critically and systematically reviewed. Based on this literature review, the following aspects can be evidenced:

- The porous structure of AAC offers several advantages in terms of lightness of the final products and both acoustic and thermal insulation, producing energy-efficient masonry components and structures, and hence benefits in terms of sustainability and building comfort.
- Mass density affects all the functional and structural properties of the AAC, but most of the properties also depend on the moisture content. This is reflected by experimental data, which allowed empirical models and relationships to be derived for structural design and assessment.
- In most of European countries, mortar for AAC masonry is arranged in thin layers (with thickness from 0.5 to 3 *mm*) and is characterized by strength values that are comparable with those of AAC blocks.

Under these conditions, AAC masonry appears to develop a rather isotropic behavior, at least in compression. The low thickness of joints also allows the mitigation of heat losses through AAC masonry, resulting into a good exploitation of the inherent thermal insulation of AAC blocks. On the contrary, different types of mortar and/or values of joint thickness are reported to have significant influence, especially on the macroscopic shear behavior of AAC masonry.

- A certain dispersion of the experimental results on masonry, sometimes controversial, has been found based on post-processing of data collected from the literature. Such an outcome is at least partially motivated by the different methods of testing used for masonry characterization.
- The amount of knowledge reviewed in this paper is being considered for preparation of state-of-the-art reports and guidelines at both national and international levels.

Further studies should deal with the experimental testing of masonry assemblages in compression and shear, in order to investigate the influence of the adopted experimental setup on macroscopic properties and their dispersion. Furthermore, the influence of some key parameters (such as block density and strength, and mortar class) on the masonry behavior should be deepened, supporting the creation of a more comprehensive database for designers and researchers.

CRediT authorship contribution statement

Elena Michelini: Writing – review & editing, Writing – original draft, Supervision, Project administration, Data curation, Conceptualization. **Daniele Ferretti:** Writing – review & editing, Writing – original draft, Project administration, Data curation, Conceptualization. **Lorenzo Miccoli:** Writing – review & editing, Writing – original draft, Data curation, Conceptualization. **Fulvio Parisi:** Writing – review & editing, Supervision, Data curation, Conceptualization.

Declaration of Competing Interest

The authors declare the following financial interests/personal relationships which may be considered as potential competing interests: Lorenzo Miccoli reports a relationship with Xella Technologie- und Forschungsgesellschaft mbH that includes: employment.

Data availability

Data will be made available on request.

References

[1] European Commission, Proposal for a Directive of the European Parliament and of the Council on energy efficiency (recast), Brussels, 2021.
[2] https://singl-market-economy.ec.europa.eu/growth/industry/sustainability/buildings-and-construction_en; (accessed: 02/05/2023).
[3] European Commission., Directive 2012/27/EU of the European Parliament and of the Council of 25 October 2012 on energy efficiency, amending Directives 2009/125/EC and 2010/30/EU and repealing Directives 2004/8/EC and 2006/32/EC, Strasbourg, 2012. http://data.europa.eu/eli/dir/2012/27/oj.
[4] C. Fudge, Designing with AAC to achieve sustainable houses, Management 9 (2011) 1–11.
[5] C. Fudge, AAC - Providing sustainable building solutions, AAC Worldw. (2022).
[6] W. van Boggelen, History of Autoclaved Aerated Concrete The short story of a long lasting building material, Aircrete Eur. (2014).
[7] F. Pacheco-Torgal, P.B. Lourenço, J.A. Labrincha, S. Kumar, P. Chindaprasirt, eds., Eco-efficient masonry bricks and blocks - Design, Properties and Durability, Woodhead Publishing, Oxford, 2015.
[8] S. Mindess, J.F. Young, D. Darwin, Concrete, Pearson Education, USA, 2003.
[9] A.W. Hendry, Masonry walls: Materials and construction, Constr. Build. Mater. 15 (2001) 323–330, https://doi.org/10.1016/S0950-0618(01)00019-8.
[10] J.A. Hess, L. Kincl, T. Amasay, P. Wolfe, Ergonomic evaluation of masons laying concrete masonry units and autoclaved aerated concrete, Appl. Ergon. 41 (2010) 477–483.
[11] R.E. Klingner, Using autoclaved aerated concrete correctly, Mason. Mag. June. (2008).
[12] H. Radhi, Viability of autoclaved aerated concrete walls for the residential sector in the United Arab Emirates, Energ. Buildings 43 (2011) 2086–2092.
[13] R.C. Valore, Cellular concretes — Part 2 physical properties, J. Proc. 50 (1954) 817–836.
[14] S. Tada, Material design of aerated concrete—An optimum performance design, Mater. Struct. 19 (1986) 21–26.
[15] F.N. Leitch, The properties of aerated concrete in service, in: Second Int. Conf. Light. Concr. London, 1980.
[16] D. Ferretti, E. Michelini, The Effect of Density on the Delicate Balance between Structural Requirements and Environmental Issues for AAC Blocks: An Experimental Investigation, Sustainability. 13 (2021) 13186.
[17] A. Keyvani, Thermal performance & fire resistance of autoclaved aerated concrete exposed humidity conditions, Int. J. Res. Eng. Technol. 3 (2014).
[18] B. Straube, P. Langer, A. Stumm, Durability of autoclaved aerated concrete, in: May 11-14, Istanbul, Available https//www.Irbnet.de/Daten/Iconda/CIB13076.pdf, 2008.
[19] A. Artino, G. Evola, G. Margani, E.M. Marino, Seismic and Energy Retrofit of Apartment Buildings through Autoclaved Aerated Concrete (AAC) Blocks Infill Walls, Sustainability. 11 (2019) 3939.
[20] M.A. Mujeebu, F. Bano, Integration of passive energy conservation measures in a detached residential building design in warm humid climate, Energy 124587 (2022).
[21] B. Rosti, A. Omidvar, N. Monghasemi, Optimal insulation thickness of common classic and modern exterior walls in different climate zones of Iran, J. Build. Eng. 27 (2020), 100954.
[22] T. Schoch, Environmental quality of buildings, AAC Worldw. (2021).
[23] H. Walther, CO2 absorption during the use phase of autoclaved aerated concrete by recarbonation, AAC Worldw. (2022).
[24] DIN 20000-404, Application of building products in structures - Part 404: Rules for the application of autoclaved aerated concrete masonry units according to DIN EN 771-4:2015-11, 2018.
[25] N.N. Lam, Recycling of AAC Waste in the Manufacture of Autoclaved Aerated Concrete in Vietnam, GEOMATE J. 20 (2021) 128–134.
[26] F. Hlawatsch, H. Aycil, J. Kropp, Autoclaved aerated concrete (AAC) rubble for new recycling building products: In dry premixed mortars for masonry, in masonry blocks and in lightweight blocks, Mauerwerk 23 (2019) 364–377.
[27] O. Kreft, Circular economy potential for autoclaved aerated concrete, Ce/Papers. 2 (2018) 465–470.
[28] R. Volk, J.J. Steins, O. Kreft, F. Schultmann, Life cycle assessment of post-demolition autoclaved aerated concrete (AAC) recycling options, Resour. Conserv. Recycl. 188 (2023), 106716.
[29] F.M. Saiyed, A.H. Makwana, J. Pitroda, C.M. Vyas, Aerated Autoclaved Concrete (AAC) Blocks: Novel Material for Construction Industry, Int. J. Adv. Res. Eng. Sci. Manag. 1 (2014) 21–32.
[30] G.I. Grinfel'd, A.A. Vishnevsky, A.S. Smirnova, Production and use of autoclaved aerated concrete in Russia, Ce/Papers. 2 (2018) 67–71. https://doi.org/https://doi.org/10.1002/cepa.883.
[31] E.A. Khalil, M.N. AbouZeid, Environmental impact of autoclaved aerated concrete in modern construction: a case study from the new Egyptian administrative capital, Int. J. Civ. Environ. Eng. 14 (2020) 1–6.
[32] L. Miccoli, Seismic performances of AAC masonry: a review of experimental and numerical approaches: Verhalten von Porenbetonmauerwerk unter seismischen Einwirkungen: eine Überprüfung der experimentellen und numerischen Ansätze, Mauerwerk 22 (2018) 314–328.
[33] A.A. Costa, A. Penna, G. Magenes, Seismic Performance of Autoclaved Aerated Concrete (AAC) Masonry: From Experimental Testing of the In-Plane Capacity of Walls to Building Response Simulation, J. Earthquake Eng. 15 (2011) 1–31, https://doi.org/10.1080/13632461003642413.
[34] M. Tomaževič, M. Gams, Shaking table study and modelling of seismic behaviour of confined AAC masonry buildings, Bull. Earthq. Eng. 10 (2012) 863–893, https://doi.org/10.1007/s10518-011-9331-x.
[35] J. Yu, J. Cao, T. Fei, Experimental study on improving seismic behavior of load-bearing masonry wall made of autoclaved aerated concrete, Trans. Tianjin Univ. 19 (2013) 419–424.
[36] ETA-17/0365, Kit for load bearing masonry subject to seismic actions – AAC masonry system, 2017.
[37] D. Ferretti, E. Michelini, N. Pongiluppi, R. Cerioni, Damage assessment of autoclaved aerated concrete buildings: some Italian case studies, Int. J. Mason. Res. Innov. 5 (2020) 279–301.
[38] Autoclaved Aerated Concrete Market Research Report by Element, by End-user, by Application, by Region - Global Forecast to 2027 - Cumulative Impact of COVID-19, 2021.
[39] N. Narayanan, K. Ramamurthy, Structure and properties of aerated concrete: A review, Cem. Concr. Compos. 22 (2000) 321–329, https://doi.org/10.1016/S0958-9465(00)00016-0.
[40] X. Qu, X. Zhao, Previous and present investigations on the components, microstructure and main properties of autoclaved aerated concrete–A review, Constr. Build. Mater. 135 (2017) 505–516.
[41] F. Vats, Autoclaved Aerated Concrete : Versatile building material, Int. J. Adv. Res. Ideas Innov. Technol. 5 (2019) 2092–2098.
[42] G. Schober, Porosity in autoclaved aerated concrete (AAC): A review on pore structure, types of porosity, measurement methods and effects of porosity on properties, in: 5th Int. Conf. Autoclaved Aerated Concr., Bydgoscsz Poland, 2011: pp. 351–359.
[43] N. Anders, Investigations about porosity analyzing of AAC, Ce/Papers. 2 (2018) 141–145.

[44] A.J. Hamad, Materials, production, properties and application of aerated lightweight concrete, Int. J. Mater. Sci. Eng. 2 (2014) 152–157.
[45] E. Holt, P. Raivio, Use of gasification residues in aerated autoclaved concrete, Cem. Concr. Res. 35 (2005) 796–802, https://doi.org/10.1016/j.cemconres.2004.05.005.
[46] Y. Song, B. Li, E.-H. Yang, Y. Liu, T. Ding, Feasibility study on utilization of municipal solid waste incineration bottom ash as aerating agent for the production of autoclaved aerated concrete, Cem. Concr. Compos. 56 (2015) 51–58.
[47] EN 771-4, Specification for masonry units - Part 4: Autoclaved aerated concrete masonry units; German version EN 771-4:2011+A1:2015, n.d.
[48] A. Kitsch, K. Rehrmann, Ytong - the Autoclaved Aerated Concrete: A brand Making History, 1, Aufl. Xella Int. Duisbg. (2012).
[49] P. Prim, F.H. Wittmann, Structure and water absorption of aerated concrete, Autoclaved Aerated Concr, Moisture Prop. (1983) 55–69.
[50] I. Kadashevich, H.J. Schneider, D. Stoyan, Statistical modeling of the geometrical structure of the system of artificial air pores in autoclaved aerated concrete, Cem. Concr. Res. 35 (2005) 1495–1502, https://doi.org/10.1016/j.cemconres.2004.10.010.
[51] C. Fudge, F. Fouad, R. Klingner, Autoclaved aerated concrete, in: Dev. Formul. Reinf. Concr., Elsevier, 2019: pp. 345–363.
[52] Y.-L. Chen, J.-E. Chang, Y.-C. Lai, M.-I.-M. Chou, A comprehensive study on the production of autoclaved aerated concrete: Effects of silica-lime-cement composition and autoclaving conditions, Constr. Build. Mater. 153 (2017) 622–629.
[53] C. Shan, Z. Yang, Z. Su, R. Rajan, X. Zhou, L. Wang, Preparation and characterization of waterproof autoclaved aerated concrete using molybdenum tailings as the raw materials, J. Build. Eng. (2022), 104036.
[54] K. Matsui, A. Ogawa, J. Kikuma, M. Tsunashima, T. Ishikawa, S. Matsuno, Influence of addition of Al compound and gypsum on tobermorite formation in autoclaved aerated concrete studied by in situ X-ray diffraction, in: 5th Int. Conf. Autoclaved Aerated Concr. Secur. a Sustain. Futur. Bydgoszcz, Pol., 2011: pp. 147–154.
[55] N. Narayanan, K. Ramamurthy, Microstructural investigations on aerated concrete, Cem. Concr. Res. 30 (2000) 457–464, https://doi.org/10.1016/S0008-8846(00)00199-X.
[56] Y. Liu, B.S. Leong, Z.-T. Hu, E.-H. Yang, Autoclaved aerated concrete incorporating waste aluminum dust as foaming agent, Constr. Build. Mater. 148 (2017) 140–147.
[57] A. Bonakdar, F. Babbitt, B. Mobasher, Physical and mechanical characterization of fiber-reinforced aerated concrete (FRAC), Cem. Concr. Compos. 38 (2013) 82–91.
[58] R.G. Mathey, W.J. Rossiter Jr., A Review of Autoclaved Aerated Concrete Products. NBSIR 87-3670, Research Information Center, National Bureau of Standards, Gaithersburg, Maryland, 1988.
[59] M. Grutzeck, S. Kwan, M. DiCola, Zeolite formation in alkali-activated cementitious systems, Cem. Concr. Res. 34 (2004) 949–955, https://doi.org/10.1016/j.cemconres.2003.11.003.
[60] R.C. Valore, Cellular concretes Part 1 composition and methods of preparation, J. Proc. 50 (1954) 773–796.
[61] M. Haas, Optimal autoclaving, in: M.C. Limbachiya, J.J. Roberts (Eds.), 4th Int. Conf. Autoclaved Aerated Concr. - Innov. Dev., Kingston University, London, 2005: pp. 67–78.
[62] S. Aroni, G.J. de Groot, M.J. Robinson, G. Svanholm, F.H. Wittman, eds., Autoclaved aerated concrete-properties, testing and design - RILEM Recommended Practice, E&FN Spon, Lodon, 1993.
[63] K. Kunchariyakun, S. Asavapisit, K. Sombatsompop, Properties of autoclaved aerated concrete incorporating rice husk ash as partial replacement for fine aggregate, Cem. Concr. Compos. 55 (2015) 11–16.
[64] B. Ma, L. Cai, X. Li, S. Jian, Utilization of iron tailings as substitute in autoclaved aerated concrete: physico-mechanical and microstructure of hydration products, J. Clean. Prod. 127 (2016) 162–171.
[65] H. El-Didamony, A.A. Amer, M.S. Mohammed, M.A. El-Hakim, Fabrication and properties of autoclaved aerated concrete containing agriculture and industrial solid wastes, J. Build. Eng. 22 (2019) 528–538.
[66] M. Albayrak, A. Yörükoğlu, S. Karahan, S. Atlıhan, H.Y. Aruntaş, İ. Girgin, Influence of zeolite additive on properties of autoclaved aerated concrete, Build. Environ. 42 (2007) 3161–3165.
[67] X. Guo, T. Zhang, Utilization of municipal solid waste incineration fly ash to produce autoclaved and modified wall blocks, J. Clean. Prod. 252 (2020), 119759.
[68] K. Ohenoja, J. Pesonen, J. Yliniemi, M. Illikainen, Utilization of fly ashes from fluidized bed combustion: A review, Sustainability. 12 (2020) 2988.
[69] A.R. Rafiza, H.Y. Chan, A. Thongtha, W. Jettipattaranat, K.L. Lim, An innovative autoclaved aerated concrete (AAC) with recycled AAC powder for low carbon construction, in, IOP Conf. Ser. Earth Environ. Sci., IOP Publishing (2019) 12050.
[70] V. Černý, R. Drochytka, P. Šebestová, Options for the implementation of new secondary raw materials in autoclaved aerated concrete, Ce/Papers. 2 (2018) 431–437, https://doi.org/10.1002/cepa.841.
[71] Y.-L. Chen, J.-E. Chang, Y.-C. Lai, M.-S. Ko, Y.-H. Chen, Recycling of steel slag fines for the production of autoclaved aerated concrete (AAC), Ce/Papers. 2 (2018) 445–449, https://doi.org/10.1002/cepa.849.
[72] M. Bao, X. Guo, H. Shi, K. Wu, X. Zhang, Utilizing municipal solid waste incineration (MSWI) fly ash as a calcium source to prepare Al-substituted tobermorite, Ce/Papers. 2 (2018) 451–456, https://doi.org/10.1002/cepa.870.
[73] A. Hauser, U. Eggenberger, T. Mumenthaler, Fly ash from cellulose industry as secondary raw material in autoclaved aerated concrete, Cem. Concr. Res. 29 (1999) 297–302, https://doi.org/10.1016/S0008-8846(98)00207-5.
[74] P. Walczak, J. Małolepszy, M. Reben, P. Szymański, K. Rzepa, Utilization of waste glass in autoclaved aerated concrete, Procedia Eng. 122 (2015) 302–309.
[75] Z. Zhang, J. Qian, C. You, C. Hu, Use of circulating fluidized bed combustion fly ash and slag in autoclaved brick, Constr. Build. Mater. 35 (2012) 109–116.
[76] H. Kurama, I.B. Topcu, C. Karakurt, Properties of the autoclaved aerated concrete produced from coal bottom ash, J. Mater. Process. Technol. 209 (2009) 767–773.
[77] N.Y. Mostafa, Influence of air-cooled slag on physicochemical properties of autoclaved aerated concrete, Cem. Concr. Res. 35 (2005) 1349–1357, https://doi.org/10.1016/j.cemconres.2004.10.011.
[78] M.S. Baspinar, I. Demir, E. Kahraman, G. Gorhan, Utilization potential of fly ash together with silica fume in autoclaved aerated concrete production, KSCE J. Civ. Eng. 18 (2014) 47–52.
[79] X. Huang, W. Ni, W. Cui, Z. Wang, L. Zhu, Preparation of autoclaved aerated concrete using copper tailings and blast furnace slag, Constr. Build. Mater. 27 (2012) 1–5.
[80] B. Yuan, C. Straub, S. Segers, Q.L. Yu, H.J.H. Brouwers, Sodium carbonate activated slag as cement replacement in autoclaved aerated concrete, Ceram. Int. 43 (2017) 6039–6047.
[81] M.W. Hussin, K. Muthusamy, F. Zakaria, Effect of mixing constituent toward engineering properties of POFA cement-based aerated concrete, J. Mater. Civil Eng. 22 (2010) 287–295.
[82] Transforming our world: the 2030 Agenda for Sustainable Development; accessible at: https://www.un.org/en/development/desa/population/migration/generalassembly/docs/globalcompact/A_RES_70_1_E.pdf.
[83] Z. Gyurkó, B. Jankus, O. Fenyvesi, R. Nemes, Sustainable applications for utilization the construction waste of aerated concrete, J. Clean. Prod. 230 (2019) 430–444.
[84] M. Kalpana, S. Mohith, Study on autoclaved aerated concrete, Mater. Today:. Proc. 22 (2020) 894–896.
[85] A. Raj, A.C. Borsaikia, U.S. Dixit, Manufacturing of Autoclaved Aerated Concrete (AAC): Present Status and Future Trends, in: Adv. Simulation, Prod. Des. Dev., Springer, 2020: pp. 825–833.
[86] EN 12602, Prefabricated reinforced components of autoclaved aerated concrete, 2016.
[87] EN 772-1, Methods of test for masonry units - Part 1: Determination of compressive strength; 2011 + A1:2015.
[88] EN 772-13, Methods of test for masonry units - Determination of net and gross dry density of masonry units (except for natural stone), 2000.
[89] EN 772-10, Methods of test for masonry units – Part 10: Determination of moisture content of calcium silicate and autoclaved aerated concrete units, 1999.
[90] EN 1352, Determination of static modulus of elasticity under compression of autoclaved aerated concrete or lightweight aggregate concrete with open structure, 1996.
[91] ASTM C469-02, Standard Test Method for Static Modulus of Elasticity and Poisson's Ratio of Concrete in Compression, 2017.
[92] EN 1351, Determination of flexural strength of autoclaved aerated concrete, 1997.
[93] ASTM C78-09, Standard Test Method for Flexural Strength of Concrete (Using Simple Beam with Third-Point Loading), 2010.
[94] EN 1015-12, Methods of test for mortar for masonry - Part 12: Determination of adhesive strength of hardened rendering and plastering mortars on substrates, 2016.
[95] EN 1052-3, Methods of test for masonry - Part 3: Determination of initial shear strength; 2002+A1:2007.
[96] EN 680, Determination of the drying shrinkage of autoclaved aerated concrete, 2005.
[97] EN 12664, Thermal performance of building materials and products - Determination of thermal resistance by means of guarded hot plate and heat flow meter methods - Dry and moist products of medium and low thermal resistance, 2001.
[98] EN 1745, Masonry and masonry products - Methods for determining thermal properties, 2020.
[99] EN ISO 12571, Hygrothermal performance of building materials and products — Determination of hygroscopic sorption properties, 2013.
[100] EN 772-11, Methods of test for masonry units - Part 11: Determination of water absorption of aggregate concrete, autoclaved aerated concrete, manufactured stone and natural stone masonry units due to capillary action and the initial rate of water absorption of clay , 2011.
[101] G. Schober, The most important aspects of microstructure influencing strength of AAC, AAC, Taylor Fr, Hal. (2005) 145–153.
[102] F. Pospisil, J. Jambor, J. Belko, Unit weight reduction of fly ash aerated concrete, Adv. Autoclaved Aerated Concr. AA Balkema. (1992) 43–52.
[103] W. Wongkeo, P. Thongsanitgarn, K. Pimraksa, A. Chaipanich, Compressive strength, flexural strength and thermal conductivity of autoclaved concrete block made using bottom ash as cement replacement materials, Mater. Des. 35 (2012) 434–439.
[104] W. Wongkeo, A. Chaipanich, Compressive strength, microstructure and thermal analysis of autoclaved and air cured structural lightweight concrete made with coal bottom ash and silica fume, Mater. Sci. Eng. A 527 (2010) 3676–3684.
[105] T. Schneider, P. Greil, G. Schober, Strength modeling of brittle materials with two- and three-dimensional pore structures, Comput. Mater. Sci 16 (1999) 98–103, https://doi.org/10.1016/S0927-0256(99)00051-8.

[106] Y. Chen, M. Peng, Y. Zhang, Y. Liu, Mechanical Properties of Autoclaved Aerated Concrete with Different Densities, Adv. Civ. Eng. Mater. 2 (2013) 441–456.
[107] J. Argudo, Evaluation and Synthesis of Experimental Data for Autoclaved Aerated Concrete, MSc Thesis, The University of Texas at Austin, 2003.
[108] J. Alexanderson, Relations between structure and mechanical properties of autoclaved aerated concrete, Cem. Concr. Res. 9 (1979) 507–514.
[109] CEB, Autoclaved Aerated Concrete. Manual of design and technology, The Construction Press, 1977.
[110] G.C. Hoff, Porosity-strength considerations for cellular concrete, Cem. Concr. Res. 2 (1972) 91–100.
[111] P. Walczak, Compressive strength of autoclaved aerated concrete: Test methods comparison, Ce/Papers. 2 (2018) 589–590.
[112] W. Mazur, Ł. Drobiec, R. Jasiński, Effects of specimen dimensions and shape on compressive strength of specific autoclaved aerated concrete, Ce/Papers. 2 (2018) 541–556.
[113] G. Svanholm, Influence of water content on properties, in: RILEM Int. Symp. Autoclaved Aerated Concr., 1983: pp. 119–129.
[114] D. Ferretti, E. Michelini, G. Rosati, Cracking in autoclaved aerated concrete: Experimental investigation and XFEM modeling, Cem. Concr. Res. 67 (2015) 156–167, https://doi.org/10.1016/j.cemconres.2014.09.005.
[115] R. Jasiński, Ł. Drobiec, W. Mazur, Validation of selected non-destructive methods for determining the compressive strength of masonry units made of autoclaved aerated concrete, Materials (Basel). 12 (2019) 389.
[116] J.E. Tanner, Design Provisions for Autoclaved Aerated Concrete (AAC) Structural Systems, The University of Texas at Austin, 2003. Ph.D. Thesis.
[117] A.T. Vermeltfoort, Shape factors for calcium silicate and aircrete based on experimental results, Mason. Int. 20 (2007) 75–84.
[118] S. Wolf, S. Wiegand, D. Stoyan, H.B. Walther, The compressive strength of AAC–a statistical investigation, Autoclaved Aerated Concr. Innov. Des. (2005) 287–295.
[119] E. Raue, E. Tartsch, P. Langer, Experimental tests into the sustained load strength of autoclaved aerated concrete, in: 4th Int. Conf. Autoclaved Aerated Concr. London, 2005: pp. 203–210.
[120] R. Jasiński, Proposal of procedure for identification of Menétrey-Willam (MW-3) plasticity surface of homogeneous and hollow masonry units, Eng. Struct. Technol. 11 (2019) 40–49.
[121] EN 1607, Thermal insulating products for building applications - Determination of tensile strength perpendicular to faces, 2013.
[122] EN 1608, Thermal insulating products for building applications - Determination of tensile strength parallel to faces, 2013.
[123] EN 679, Determination of the compressive strength of autoclaved aerated concrete, 2005.
[124] ACI Committee 523, ACI 523.4R-09. Guide for Design and Construction with Autoclaved Aerated Concrete Panels., 2009.
[125] NEN 3838 - Gasbetonproducten - Aerated concrete products, NNI (Netherlands Normalisatie-Instituut), Delft, The Netherlands, 1987.
[126] N. Isu, S. Teramura, H. Ishida, T. Mitsuda, Influence of quartz particle size on the chemical and mechanical properties of autoclaved aerated concrete (II) fracture toughness, strength and micropore, Cement and Concrete Research 25 (1995) 249–254.
[127] F.H. Wittmann, I. Gheorghita, Fracture toughness of autoclaved aerated concrete, Cem. Concr. Res. 14 (1984) 369–374.
[128] E. Brühwiler, J. Wang, F.H. Wittmann, Fracture of AAC as influenced by specimen dimension and moisture, J. Mater. Civ. Eng. 2 (1990) 136–146.
[129] B. Trunk, G. Schober, A.K. Helbling, F.H. Wittmann, Fracture mechanics parameters of autoclaved aerated concrete, Cem. Concr. Res. 29 (1999) 855–859, https://doi.org/10.1016/S0008-8846(99)00059-9.
[130] E. Michelini, D. Ferretti, M. Pizzati, The influence of density on the fracture energy of AAC: From experimental investigation to the calibration of a cohesive law, Constr. Build. Mater. 400 (2023) 13254.
[131] H.D. Jeong, H. Takahashi, S. Teramura, Low temperature fracture behaviour and AE characteristics of autoclaved aerated concrete (AAC), Cem. Concr. Res. 17 (1987) 743–754.
[132] GB/T 17431.2, Lightweight aggregates and its test methods. Part 2: Test methods for lightweight aggregates, 2010.
[133] K. Ramamurthy, N. Narayanan, Influence of composition and curing on drying shrinkage of aerated concrete, Mater. Struct. 33 (2000) 243–250.
[134] A. Georgiades, C.H. Ftikos, J. Marinos, Effect of micropore structure on autoclaved aerated concrete shrinkage, Cem. Concr. Res. 21 (1991) 655–662.
[135] H. Ziembika, Effect of micropore structure on cellular concrete shrinkage, Cem. Concr. Res. 7 (1977) 323–332.
[136] P. Schubert, Shrinkage behaviour of aerated concrete, Autoclaved Aerated Concr, Moisture Prop. Amsterdam Elsevier. (1983) 207–217.
[137] M.R. Jones, M.J. McCarthy, A. McCarthy, Moving fly ash utilization in concrete forward: A UK perspective, in: 2003 Int. Ash Util. Symp., 2003: pp. 20–22.
[138] I. Asadi, P. Shafigh, Z.F.B.A. Hassan, N.B. Mahyuddin, Thermal conductivity of concrete–A review, J. Build. Eng. 20 (2018) 81–93.
[139] L. Miccoli, P. Fontana, N. Silva, A. Klinge, C. Cederqvist, O. Kreft, D. Qvaeschning, C. Sjöström, Composite UHPC-AAC/CLC facade elements with modified interior plaster for new buildings and refurbishment. Materials and production technology, J. Facade Des. Eng. 3 (2015) 91–102, https://doi.org/10.3233/fde-150029.
[140] M. Jerman, M. Keppert, J. Výborný, R. Černý, Hygric, thermal and durability properties of autoclaved aerated concrete, Constr. Build. Mater. 41 (2013) 352–359.
[141] R. Yang, J. Zhu, Z. Wu, Z. Wu, M. Li, C. Peng, Thermal insulation and strength of autoclaved light concrete, J. Wuhan Univ. Technol. Sci. Ed. 26 (2011) 132–136.
[142] B. Straube, H. Walther, AAC with low thermal conductivity, Cem Wapno Bet. (2011) 78–80.
[143] G. Chen, F. Li, P. Jing, J. Geng, Z. Si, Effect of pore structure on thermal conductivity and mechanical properties of Autoclaved Aerated Concrete, Materials (Basel) 14 (2021) 339, https://doi.org/10.1016/j.conbuildmat.2021.123572.
[144] EN ISO, 6946, Building components and building elements - Thermal resistance and thermal transmittance -, Calculation method (2007).
[145] EN ISO 10456, Building materials and products - Hygrothermal properties - Tabulated design values and procedures for determining declared and design thermal values (ISO 10456:2007 + Cor. 1:2009), 2009.
[146] T. Schoch, O. Kreft, The influence of moisture on the thermal conductivity of AAC, in: 5th Int. Conf. Autoclaved Aerated Concr. “Securing a Sustain. Futur. to Be Held Bydgoszcz to Celebr. 60 Years AAC Exp. Poland, Bydgoszcz, 2011: pp. 44–48.
[147] J.P. Laurent, C. Guerre-Chaley, Influence of water content and temperature on the thermal conductivity of autoclaved aerated concrete, Mater. Struct. 28 (1995) 464–472.
[148] A.G. Loudon, The effect of moisture content on thermal conductivity, Autoclaved Aerated Concr, Moisture Prop. Dev. Civ. Eng. 6 (1983) 131–142.
[149] H.-Q. Jin, X.-L. Yao, L.-W. Fan, X. Xu, Z.-T. Yu, Experimental determination and fractal modeling of the effective thermal conductivity of autoclaved aerated concrete: Effects of moisture content, Int. J. Heat Mass Transf. 92 (2016) 589–602.
[150] EN 12667, Thermal performance of building materials and products - Determination of thermal resistance by means of guarded hot plate and heat flow meter methods. Products of high and medium thermal resistance, 2002.
[151] DIN 52612, Testing of Thermal Insulating Materials; Determination of Thermal Conductivity by the Guarded Hot Plate Apparatus; Test Procedure and Evaluation, 1.
[152] S. Tada, S. Nakano, Microstructural approach to properties of moist cellular concrete, Proc. Autoclaved Aerated Concr. Moisture Prop. Amsterdam Elsevier. (1983) 71–89.
[153] C. Boutin, Conductivité thermique du béton cellulaire autoclavé: modélisation par méthode autocohérente, Mater. Struct. 29 (1996) 609–615.
[154] A. Różycka, W. Pichór, Effect of perlite waste addition on the properties of autoclaved aerated concrete, Constr. Build. Mater. 120 (2016) 65–71.
[155] EN 998-2, Specification for mortar for masonry – Part 2: Masonry mortar; German version EN 998 2:2016, 2017.
[156] EN 1015-11:2020-01, Methods of test for mortar for masonry - Part 11: Determination of flexural and compressive strength of hardened mortar; German version EN 1015-11:2019, 2020.
[157] EN 1015-10:2007-05, Methods of test for mortar for masonry - Part 10: Determination of dry bulk density of hardened mortar; German version EN 1015-10:1999+A1:2006, 2007.
[158] EN 1015-6: 2007-05, Methods of test for mortar for masonry - Part 6: Determination of bulk density of fresh mortar; German version EN 1015-6:1998+A1:2006, 2007.
[159] EN 1015-3:2007-05, Methods of test for mortar for masonry - Part 3: Determination of consistence of fresh mortar (by flow table); German version EN 1015-3:1999+A1:2004+A2:2006, 2007.
[160] EN 1015-1, Methods of test for mortar for masonry - Part 1: Determination of particle size distribution (by sieve analysis), 2007.
[161] EN 13501-1, Fire classification of construction products and building elements - Part 1: Classification using data from reaction to fire tests, 2019.
[162] ESR-1371, ICC ES Report - Autoclaved Aerated Concrete block masonry units, 2004.
[163] R. Jasinski, I. Galman, Strength of Unreinforced Joints of Masonry Walls Made of AAC Masonry Units, in: IOP Conf. Ser. Mater. Sci. Eng., IOP Publishing, 2019, p. 32075.
[164] EN 1996-1-1, Eurocode 6 - Design of masonry structures - Part 1-1: General rules for reinforced and unreinforced masonry structures; 2005 + A1:2012.
[165] EN 1052-1, Methods of test for masonry - Determination of compressive strength; German version EN 1052 1:1998.
[166] L. Drobiec, R. Jasiński, T. Rybarczyk, The influence of the type of mortar on the compressive behaviour of walls made of Autoclaved Aerated Concrete (AAC), in: M.R.V. Claudio Modena, F. da Porto (Ed.), 16th Int. Brick Block Mason. Conf., Padova (Italy), 2016: pp. 1531–1538.
[167] DIN EN 1996-1-1/NA:2019-12, National Annex - Nationally determined parameters - Eurocode 6: Design of masonry structures - Part 1-1: General rules for reinforced and unreinforced masonry structures;, 2012.
[168] ASTM C1314-18, Standard Test Method for Compressive Strength of Masonry Prisms, 2018.
[169] Y.A. Daou, Compressive Strength of Autoclaved Aerated Concrete Blockwork, J. Appl. Sci. 1 (2001) 385–390.
[170] D. Ferretti, E. Michelini, G. Rosati, Mechanical characterization of autoclaved aerated concrete masonry subjected to in-plane loading: Experimental investigation and FE modeling, Constr. Build. Mater. 98 (2015) 353–365, https://doi.org/10.1016/j.conbuildmat.2015.08.121.
[171] R. Jasiński, Identification of stress states in compressed masonry walls using a non-destructive technique (NDT), Materials (Basel). 13 (2020) 2852.
[172] R. Jasiński, K. Stebel, P. Kielan, Use of the AE effect to determine the stresses state in AAC masonry walls under compression, Materials (Basel). 14 (2021) 3459.
[173] R. Jasiński, Ł. Drobiec, Study of autoclaved aerated concrete masonry walls with horizontal reinforcement under compression and shear, Procedia Eng. 161 (2016) 918–924.

[174] R. Jasiński, Ł. Drobiec, Comparison research of bed joints construction and bed joints reinforcement on shear parameters of AAC masonry walls, J. Civ. Eng. Archit. 10 (2016) 1329–1343.
[175] R. Jasiński, Ł. Drobiec, Effects of Technology of Placing Different Types of Reinforcement in Bed Joints on Compressive and Shear Strength of AAC Masonry Walls IOP Conf, Ser. Mater. Sci. Eng. 471 (2019).
[176] EN 1052-2, Methods of test for masonry - Part 2: Determination of flexural strength; 2016 + AC: 2017.
[177] A. Piekarczyk, Flexural strength of AAC masonry with bed joint reinforcement, Ce/Papers. 2 (2018) 389–396.
[178] A. Ahmed, A. Fried, Flexural strength of low density blockwork, Constr. Build. Mater. 35 (2012) 516–520.
[179] M. Al-Shaleh, E.K. Attiogbe, Flexural strength characteristics of non-load bearing masonry walls in Kuwait, Mater. Struct. 30 (1997) 277.
[180] N. Augenti, F. Parisi, Teoria e tecnica delle strutture in muratura: Analisi e progettazione, HOEPLI EDITORE, 2019.
[181] A. Rosti, A. Penna, M. Rota, G. Magenes, In-plane cyclic response of low-density AAC URM walls, Mater. Struct. 49 (2016) 4785–4798, https://doi.org/10.1617/s11527-016-0825-5.
[182] N. Augenti, F. Parisi, Constitutive modelling of tuff masonry in direct shear, Constr. Build. Mater. 25 (2011) 1612–1620.
[183] J. Segura, E. Bernat, V. Mendizábal, L. Pelà, P. Roca, L. Gil, Experimental comparison of two testing setups for characterizing the shear mechanical properties of masonry, J. Build. Eng. 44 (2021), 103277.
[184] A. Bhosale, N.P. Zade, R. Davis, P. Sarkar, Experimental investigation of autoclaved aerated concrete masonry, J. Mater. Civil Eng. 31 (2019) 4019109.
[185] A. Raj, A.C. Borsaikia, U.S. Dixit, Bond strength of Autoclaved Aerated Concrete (AAC) masonry using various joint materials, J. Build. Eng. 28 (2020), 101039.
[186] U. Schmidt, I. Beer, W. Brameshuber, Tests on the Load Bearing Behaviour of Masonry Shear Walls. Calgary: Department of Civil Engineering, 2005, in: 10th Can. Mason. Symp. Banff, Alberta, Canada, 2005: pp. 704–713.
[187] DIN 18555-5, Testing of mortars containing mineral binders; hardened mortars; determination of bond shear strength of masonry mortars, 1986.
[188] M. Vanheukelom, R. Das, H. Degée, B. Vandoren, Experimental Characterization of the Initial Shear Strength of Composite Masonry including AAC Blocks and DPC Layers, Sustainability. 13 (2021) 12749.
[189] ASTM E-519-2, No TitleStandard Test Method for Diagonal Tension (Shear) in Masonry Assemblages, 2015.
[190] J. Kubica, I. Galman, Comparison of two ways of AAC block masonry strengthening using CFRP strips-diagonal compression test, Procedia Eng. 193 (2017) 42–49.